



# A Trefftz-discontinuous Galerkin method for time-harmonic elastic wave problems

Long Yuan<sup>1</sup> · Yang Liu<sup>2</sup>

Received: 15 July 2018 / Revised: 26 March 2019 / Accepted: 22 May 2019 / Published online: 3 June 2019  
© SBMAC - Sociedade Brasileira de Matemática Aplicada e Computacional 2019

## Abstract

In this paper, we develop a plane wave discontinuous Galerkin method combined with local spectral element method for the elastic wave propagation in two and three space dimensions. We derive the error estimates of the approximation solutions in the mesh-dependent norm and the mesh-independent norm. Some dependence of the error bounds on the orders  $q$  of local spectral elements and the number  $p$  of plane wave propagation directions is given. Numerical results assess the validity of the theoretical results and indicate that the resulting approximate solutions generated by the PWDG–LSFE possess high accuracy.

**Keywords** Elastic waves · Nonhomogeneous · Local spectral element · Plane wave discontinuous Galerkin · Plane wave basis functions · Error estimates

**Mathematics Subject Classification** 65N30 · 65N55

## 1 Introduction

The plane wave method turned out to be an efficient and popular method for solving wave propagation problems in time-harmonic regime at medium and high frequencies. The main

---

Communicated by Frederic Valentin.

---

L. Yuan was supported by China NSF under the grant 11501529, Qindao applied basic research project under grant 17-1-1-9-jch and Scientific Research Foundation of Shandong University of Science and Technology for Recruited Talents. Y. Liu was supported by China NSF under the Grant 11571196 and the Science Challenge Program (no. TZ2018002).

---

✉ Long Yuan  
yuanlong@lsec.cc.ac.cn

Yang Liu  
liuyang@lsec.cc.ac.cn

<sup>1</sup> College of Mathematics and Systems Science, Shandong University of Science and Technology, Qingdao 266590, People's Republic of China

<sup>2</sup> Institute of Applied Physics and Computational Mathematics, Beijing 100094, People's Republic of China

feature of the method is to choose plane wave solutions of the governing differential equation without boundary conditions as the basis functions. The plane wave method was first introduced to solve Helmholtz equations and was then extended to solve the Maxwell equations and time-harmonic elastic wave problems. Examples of this approach include the partition of unity-type method (Perrey-Debain et al. 2003a, b), the plane wave partition of unity finite-element method (El Kacimi and Laghrouche 2009, 2010), the variational theory of complex rays (VTCR) (Riou et al. 2008, 2012; Yuan and Hu 2018), the ultra weak variational formulation (UWVF) (Cessenat and Despres 1998, 2003; Huttunen et al. 2004, 2007; Luostari 2013), the plane wave discontinuous Galerkin (PWDG) method (Gittelsohn et al. 2009; Hiptmair et al. 2013, 2016; Moiola 2013; Yuan 2019; Yuan and Hu 2019) and the plane wave least-squares (PWLS) method (Monk and Wang 1999; Hu and Yuan 2014a, b, 2018; Peng et al. 2018; Yuan et al. 2016) and the plane wave least-squares combined with local spectral finite-element (PWLS–LSFE) method (Hu and Yuan 2018).

The UWVF method was developed for the Helmholtz equations (Cessenat and Despres 1998, 2003) and for Maxwell's equations (Cessenat 1996; Cessenat and Despres 1998; Huttunen et al. 2007; Huttunen and Monk 2007). The UWVF method is derived from non-overlapping domain decomposition with mixed interface conditions. The PWDG method developed in Gittelsohn et al. (2009), Hiptmair et al. (2011, 2013, 2016) was derived from standard discontinuous Galerkin (DG) methods. We see that the choice  $\alpha = \beta = \delta = 1/2$  of flux parameters gives rise to the original UWVF introduced in Cessenat (1996), Cessenat and Despres (1998). The PWLS method, first put forward in Monk and Wang (1999), starts from a minimization problem in which the objective functional contains the jumps of the standard traces on local interfaces and a relaxation factor. To our knowledge, the existing numerical results indicate that the PWDG method can generate approximate solutions with higher accuracy for the homogeneous governing equations with real coefficients.

The UWVF method was extended to solve homogeneous elastic wave problems in Huttunen et al. (2004), Luostari (2013). The studies (Huttunen et al. 2004; Luostari 2013) were devoted to approximating the  $S$ - and  $P$ -wave components of the analytic solution in a balanced way for the accuracy and stability in two-dimensional case. For the UWVF method, the traction of the approximation solution on the boundaries of every elements is chosen as the unknowns, and the conjugation of each traction has to be defined by introducing an additional mappings. The displacement field on the skeleton of the mesh can be recovered by the unknowns.

Since plane wave basis functions on each element are solutions of the *homogeneous* governing equations without boundary condition, it was pointed out in (Hiptmair et al. 2011, p. 265) that *In particular, in Gittelsohn et al. (2009), an  $h$ -version error analysis for the PWDG method applied to the two-dimensional (2D) inhomogeneous Helmholtz problem was carried out. In that case, independent of how many plane waves are used in the local approximation spaces, only first-order convergence can be achieved in general. In the recently published work (Hu and Yuan 2018), the plane wave method combined with local spectral elements (PWLS–LSFE) for the discretization of such nonhomogeneous equations was firstly proposed. The key ingredient of this method is to first solve a series of nonhomogeneous local problems on auxiliary smooth subdomains by the spectral element method, and then discretize the resulting (locally homogeneous) residue problem on the global solution domain by the standard plane wave method. The numerical results show that the approximate solutions generated by the PWLS–LSFE method possess satisfactory error estimates with high  $h$ -convergence orders.*

In this paper, we are mainly interested in extending the PWDG method combined with local spectral elements (PWDG–LSFE) to discretize the nonhomogeneous elastic wave prob-

lems in two and three dimensions. We derive error estimates of the approximate solutions generated by the proposed method. To our knowledge, there are no error estimates with high  $h$ -convergence orders for the plane wave methods solving the nonhomogeneous elastic wave equations in the existing literature. In addition, in the error estimates, some dependence of the error bounds on the orders  $q$  of local spectral elements and also on the number  $p$  of plane wave propagation directions is explicitly given. We can also extend the results to other plane wave methods for the considered model.

Numerical experiments verify the validity of the theoretical results and indicate that the resulting approximate solutions generated by the PWDG–LSFE possess the high accuracies. To obtain an approximate solution with high accuracy but without superfluous cost, some balance relations satisfied by the parameters  $m$  and  $q$  are discussed. Moreover, the approximate solutions generated by the proposed method have high accuracy when the wavenumber increases for the fixed value  $\omega h$ .

The paper is organized as follows: In Sect. 2, we introduce the linear time-harmonic equations of elasticity, together with triangulation of the computational domain. In Sect. 3, we present the proposed PWDG–LSFE for elastic wave problems. In Sect. 4, we explain how to discretize the variational problem. In Sect. 5, we give error estimates for the approximate solutions of the nonhomogeneous equations. Finally, in Sect. 6, we report some numerical results to confirm the effectiveness of the methods.

## 2 Description of the underlying time-harmonic elastic wave propagation

In this section, we shall recall the problem to be solved.

The considered original problem is based on a triangulation of the solution domain. Let  $\Omega$  be the underlying domain in  $\mathbb{R}^d$  ( $d = 2, 3$ ). For convenience, assume that  $\Omega$  is a bounded polygon or polyhedron. Let  $\Omega$  be divided into the union of some subdomains in the sense that

$$\bar{\Omega} = \bigcup_{k=1}^N \bar{\Omega}_k, \quad \Omega_l \cap \Omega_j = \emptyset \quad \text{for } l \neq j,$$

where each  $\Omega_k$  is a polygon for two-dimensional case or polyhedron for three-dimensional case. Let  $\mathcal{T}_h$  denote the triangulation comprised of the elements  $\{\Omega_k\}$ , where  $h$  is the mesh-width of the triangulation. As usual, we assume that  $\mathcal{T}_h$  is quasi-uniform and regular. We denote the diameter of a simplex  $\Omega_k \in \mathcal{T}_h$  by  $h_k$  and the diameter of its largest inscribed disc or sphere by  $\rho_k$ . The conditions that  $\mathcal{T}_h$  is quasi-uniform and regular mean that there exists a constant  $C$  independent of  $\Omega_k$  and  $\mathcal{T}_h$  such that for all  $\Omega_k \in \mathcal{T}_h$  and all  $\mathcal{T}_h$ ,

$$\frac{h_K}{\rho_K} \leq C \quad \text{and} \quad \frac{h}{h_K} \leq C,$$

respectively.

Define

$$\Gamma_{lj} = \partial\Omega_l \cap \partial\Omega_j, \quad \text{for } l \neq j$$

and

$$\gamma_k = \overline{\Omega}_k \cap \partial\Omega \quad (k = 1, \dots, N), \quad \gamma = \bigcup_{k=1}^N \gamma_k.$$

We denote by  $\mathcal{F}_h = \bigcup_k \partial\Omega_k$  the skeleton of the mesh, and set  $\mathcal{F}_h^B = \mathcal{F}_h \cap \partial\Omega$  and  $\mathcal{F}_h^I = \mathcal{F}_h \setminus \mathcal{F}_h^B$ . Then, we want to compute a numerical approximation of the time-harmonic displacement vector  $\mathbf{u}$  satisfying the Navier equation [refer to Graff (1991)]:

$$\mu \Delta \mathbf{u} + (\lambda + \mu) \nabla(\nabla \cdot \mathbf{u}) + \omega^2 \rho \mathbf{u} = \mathbf{f} \quad \text{in } \Omega \tag{2.1}$$

with the lowest-order absorbing boundary condition (see Huttunen et al. (2004))

$$\mathbf{T}^{(n)}(\mathbf{u}) - i\eta \mathbf{u} = \mathbf{g} \quad \text{on } \gamma = \partial\Omega. \tag{2.2}$$

Here, the Lamé constants  $\lambda$  and  $\mu$  can be expressed by means of the Poisson ratio  $\nu$  and Young’s modulus  $E$  as follows.

$$\mu = \frac{E}{2(1 + \nu)}, \quad \lambda = \frac{E\nu}{(1 + \nu)(1 - 2\nu)}.$$

The density of the medium  $\rho$  is independent of position,  $\omega$  is the angular frequency of the field. All these coefficients are assumed to be constant in the whole domain. We shall assume that  $\mathbf{g} \in (L^2_{\mathbf{T}}(\partial\Omega))^d$ , and the traction operator  $\mathbf{T}^{(n)}$  defined on a curve  $S$  ( $d = 2$ ) or a surface ( $d = 3$ ) with a unit normal  $\mathbf{n}$  is

$$\mathbf{T}^{(n)}(\mathbf{u}) = 2\mu \frac{\partial \mathbf{u}}{\partial \mathbf{n}} + \lambda \mathbf{n} \nabla \cdot \mathbf{u} + \mu \mathbf{n} \times (\nabla \times \mathbf{u}). \tag{2.3}$$

Define the wave speed  $C_P$  for the  $P$ -wave and the wave speed  $C_S$  for the  $S$ -wave as follows ( $P$ -wave and  $S$ -wave will be introduced in Sect. 4).

$$C_P = \sqrt{\frac{\lambda + 2\mu}{\rho}} \quad \text{and} \quad C_S = \sqrt{\frac{\mu}{\rho}}.$$

Moreover, a positive definite real-valued matrix function  $\sigma$  on the external boundary  $\gamma$  is defined by

$$\eta = \omega\rho(C_P \mathbf{n} \otimes \mathbf{n} + C_S \mathbf{s} \otimes \mathbf{s}) \tag{2.4}$$

for two-dimensional case and by

$$\eta = \omega\rho(C_P \mathbf{n} \otimes \mathbf{n} + C_S \mathbf{s}_1 \otimes \mathbf{s}_1 + C_S \mathbf{s}_2 \otimes \mathbf{s}_2) \tag{2.5}$$

for three-dimensional case, respectively. Here,  $\mathbf{s}$  and  $\mathbf{s}_1, \mathbf{s}_2$  are the tangential vectors to the boundary, and  $\otimes$  denotes the outer product so that  $\mathbf{n} \otimes \mathbf{n} = \mathbf{nn}^T$ .

For each element  $\Omega_k$ , let  $\mathbf{u}|_{\Omega_k} = \mathbf{u}_k$  ( $k = 1, \dots, N$ ). Then, the reference problem (2.1)–(2.2) to be solved consists of finding the local displacement vector  $\mathbf{u}_k$  such that

$$\mu \Delta \mathbf{u}_k + (\lambda + \mu) \nabla(\nabla \cdot \mathbf{u}_k) + \omega^2 \rho \mathbf{u}_k = \mathbf{f} \quad \text{in } \Omega_k, \tag{2.6}$$

and the interface conditions (note that  $\mathbf{n}_l = -\mathbf{n}_j$ )

$$\begin{cases} \mathbf{u}_l = \mathbf{u}_j \\ \mathbf{T}^{(\mathbf{n}_l)}(\mathbf{u}_l) = -\mathbf{T}^{(\mathbf{n}_j)}(\mathbf{u}_j) \end{cases} \quad \text{on } \Gamma_{lj} \quad (l < j; l, j = 1, 2, \dots, N). \tag{2.7}$$

The boundary condition becomes

$$\mathbf{T}^{(n)}(\mathbf{u}_k) - i\eta\mathbf{u}_k = \mathbf{g}_k \quad \text{on } \gamma_k = \partial\Omega_k \cap \gamma. \tag{2.8}$$

In the next section, we introduce a new variational formulation of the elastic wave problems (2.6), (2.7), and (2.8).

### 3 The PWDG–LSFE for the nonhomogeneous time-harmonic elastic wave equations

In this section, we shall detail the PWDG–LSFE method for the elastic wave problems. As in Hu and Yuan (2018), the basic idea is to decompose the solution  $\mathbf{u}$  of (2.1), (2.2) into

$$\mathbf{u} = \mathbf{u}^{(1)} + \mathbf{u}^{(2)}, \tag{3.1}$$

where  $\mathbf{u}^{(1)}$  is a particular solution of (2.6) without the primal boundary condition, and  $\mathbf{u}^{(2)}$  satisfies a locally homogeneous elastic wave equation.

#### 3.1 Local variational formulation for the local nonhomogeneous problems

For each element  $\Omega_k$ , let  $\Omega_k^*$  be a fictitious domain that has almost the same size with  $\Omega_k$  and contains  $\Omega_k$  as its subdomain. We choose each fictitious domain  $\Omega_k^*$  so that it possesses sufficiently smooth boundary  $\partial\Omega_k^*$ . A natural way is to choose  $\Omega_k^*$  as a disc for the two-dimensional case or a sphere for the three-dimensional case that has the same center  $O_k$  with  $\Omega_k$  and has the radius  $r_k = \max\{\text{dist}(O_k, V_k^r)\}$ , where  $V_k^r$  denotes a vertex of  $\Omega_k$ .

Let  $\mathbf{u}^{(1)} \in \mathbf{L}^2(\Omega)$  be defined as  $\mathbf{u}^{(1)}|_{\Omega_k} = \mathbf{u}_k^{(1)}|_{\Omega_k}$  for each  $\Omega_k$ , where  $\mathbf{u}_k^{(1)} \in \mathbf{H}^1(\Omega_k^*)$  satisfies the nonhomogeneous local elastic wave equation on the fictitious domain  $\Omega_k^*$ :

$$\begin{cases} \mu\Delta\mathbf{u}_k^{(1)} + (\lambda + \mu)\nabla(\nabla \cdot \mathbf{u}_k^{(1)}) + \omega^2\rho\mathbf{u}_k^{(1)} = \mathbf{f} & \text{in } \Omega_k^* \\ \mathbf{T}^{(n_k)}(\mathbf{u}_k^{(1)}) - i\eta\mathbf{u}_k^{(1)} = \mathbf{0} & \text{on } \partial\Omega_k^* \end{cases} \quad (k = 1, 2, \dots, N). \tag{3.2}$$

The variational problem of (3.2) is to find  $\mathbf{u}_k^{(1)} \in \mathbf{H}^1(\Omega_k^*)$  such that

$$\begin{cases} \int_{\Omega_k^*} (-\lambda \nabla \cdot \mathbf{u}_k^{(1)} \overline{\nabla \cdot \mathbf{v}_k} - 2\mu \varepsilon(\mathbf{u}_k^{(1)}) \cdot \overline{\varepsilon(\mathbf{v}_k)} + \omega^2 \rho \mathbf{u}_k^{(1)} \cdot \overline{\mathbf{v}_k}) \, d\mathbf{x} + \int_{\partial\Omega_k^*} i \eta \mathbf{u}_k^{(1)} \cdot \overline{\mathbf{v}_k} \, dS \\ = \int_{\Omega_k^*} \mathbf{f} \cdot \overline{\mathbf{v}_k} \, d\mathbf{x}, \quad \forall \mathbf{v}_k \in \mathbf{H}^1(\Omega_k^*) \quad (k = 1, 2, \dots, N), \end{cases} \tag{3.3}$$

where the strain tensor is defined by  $\varepsilon(\mathbf{v}) := \frac{1}{2}(\nabla\mathbf{v} + \nabla\mathbf{v}^T)$ .

When  $\mathbf{f}$  satisfies  $\mathbf{f} \in \mathbf{L}^2(\Omega_k^*)$ , the variational problem (3.3) possesses a unique solution  $\mathbf{u}_k^{(1)} \in \mathbf{H}^2(\Omega_k^*)$  [see (Cummings and Feng 2006, Theorem 2)].

#### 3.2 Global variational formulation for the residual and global homogeneous problem

It is easy to see that  $\mathbf{u}^{(2)} = \mathbf{u} - \mathbf{u}^{(1)}$  is uniquely determined by the following homogeneous elastic wave equations:

$$\mu\Delta\mathbf{u}^{(2)} + (\lambda + \mu)\nabla(\nabla \cdot \mathbf{u}^{(2)}) + \omega^2\rho\mathbf{u}^{(2)} = \mathbf{0} \quad \text{in } \Omega_k \quad (k = 1, 2, \dots, N), \tag{3.4}$$

with the following boundary condition on  $\gamma$  and the interface conditions on  $\Gamma_{lj}$  ( $l < j$ ;  $l, j = 1, \dots, N$ ):

$$\begin{cases} [[\mathbf{T}^{(n)}(\mathbf{u}^{(1)} + \mathbf{u}^{(2)})]] = [[\mathbf{u}^{(1)} + \mathbf{u}^{(2)}]] = \mathbf{0}, & \text{on } \Gamma_{lj}, \quad (l < j; l, j = 1, 2, \dots, N) \\ \mathbf{T}^{(n)}(\mathbf{u}^{(1)} + \mathbf{u}^{(2)}) - i\eta(\mathbf{u}^{(1)} + \mathbf{u}^{(2)}) = \mathbf{g} & \text{on } \gamma = \partial\Omega, \end{cases} \quad (3.5)$$

where  $[[\mathbf{T}^{(n)}(\mathbf{u})]] = \mathbf{T}^{(n_l)}(\mathbf{u}_l) + \mathbf{T}^{(n_j)}(\mathbf{u}_j)$ .

Define the stress tensor

$$\boldsymbol{\sigma}(\mathbf{u}) = (\lambda \nabla \cdot \mathbf{u})I_d + 2\mu\boldsymbol{\varepsilon}(\mathbf{u}), \quad (3.6)$$

where  $I_d$  is the identity matrix. Note that the stress tensor is symmetric. By direct calculation, we can obtain

$$\begin{aligned} \boldsymbol{\sigma}(\mathbf{u})\mathbf{n} &= \mathbf{T}^{(n)}(\mathbf{u}), \\ \text{and } \nabla \cdot \boldsymbol{\sigma}(\mathbf{u}) &= \mu\Delta\mathbf{u} + (\lambda + \mu)\nabla(\nabla \cdot \mathbf{u}). \end{aligned}$$

Then the original problem (2.1, 2.2) can be rewritten as a first-order system

$$\begin{cases} \boldsymbol{\sigma}(\mathbf{u}) = (\lambda \nabla \cdot \mathbf{u})I_d + 2\mu\boldsymbol{\varepsilon}(\mathbf{u}) & \text{in } \Omega, \\ \nabla \cdot \boldsymbol{\sigma}(\mathbf{u}) + \omega^2\rho\mathbf{u} = \mathbf{f} & \text{in } \Omega, \\ \boldsymbol{\sigma}(\mathbf{u})\mathbf{n} - i\eta\mathbf{u} = \mathbf{g} & \text{on } \gamma = \partial\Omega. \end{cases} \quad (3.7)$$

Define the averages and jumps across a common face  $\partial\Omega_l \cap \partial\Omega_j$  by

$$\begin{aligned} \text{the averages: } \{\{\mathbf{u}\}\} &:= \frac{\mathbf{u}_l + \mathbf{u}_j}{2}, \quad \{\{\boldsymbol{\sigma}(\mathbf{u})\}\} := \frac{\boldsymbol{\sigma}(\mathbf{u}_l) + \boldsymbol{\sigma}(\mathbf{u}_j)}{2}, \\ \text{the jumps: } [[[\mathbf{u}]]] &:= \mathbf{u}_l \otimes \mathbf{n}_l + \mathbf{u}_j \otimes \mathbf{n}_j, \quad [[[\boldsymbol{\sigma}(\mathbf{u})]]] = \boldsymbol{\sigma}(\mathbf{u}_l)\mathbf{n}_l + \boldsymbol{\sigma}(\mathbf{u}_j)\mathbf{n}_j. \end{aligned} \quad (3.8)$$

To derive the PWDG–LSFE method, define the Trefftz spaces as follows:

$$\mathbf{V}(\Omega_k) = \{\mathbf{v} \in H^1(\Omega_k); \nabla \cdot \boldsymbol{\sigma}(\mathbf{v}) + \omega^2\rho\mathbf{v} = \mathbf{0}\}, \quad (3.9)$$

and

$$\mathbf{V}(\mathcal{T}_h) = \{\mathbf{v} \in (L^2(\Omega))^d; \mathbf{v} \in \mathbf{V}(\Omega_k) \text{ on each } \Omega_k\}.$$

Define the approximation  $\mathbf{u}_h$  of the original problem by  $\mathbf{u}_h = \mathbf{u}_h^{(1)} + \mathbf{u}_h^{(2)}$ , where  $\mathbf{u}_h^{(1)}$  and  $\mathbf{u}_h^{(2)}$  defined in next section are the approximation of (3.3) and the plane wave approximation of (3.4, 3.5), respectively.

Integrating by parts the second equation of (3.7) for every  $\Omega_k \in \mathcal{T}_h$ , we get the equation of the vector-valued function  $\mathbf{u} \in \mathbf{V}(\Omega_k)$

$$\int_{\Omega_k} (-\boldsymbol{\sigma}(\mathbf{u}) : \overline{\nabla\mathbf{v}} + \omega^2\rho\mathbf{u} \cdot \overline{\mathbf{v}})dx + \int_{\partial\Omega_k} \boldsymbol{\sigma}(\mathbf{u})\mathbf{n} \cdot \overline{\mathbf{v}}dS = \int_{\Omega_k} \mathbf{f} \cdot \overline{\mathbf{v}}dx, \quad \forall \mathbf{v} \in \mathbf{V}(\Omega_k). \quad (3.10)$$

Here, the matrix inner product  $A : B$  is

$$A : B = \sum_{k=1}^M \sum_{l=1}^M a_{kl}b_{kl},$$

where  $A = (a_{kl})_{M \times M}$  and  $B = (b_{kl})_{M \times M}$ .

By the direct computation, for any sufficiently smooth functions  $\mathbf{v}$  and  $\mathbf{w}$ , the following relation holds

$$\boldsymbol{\sigma}(\mathbf{v}) : \nabla \mathbf{w} = \lambda \nabla \cdot \mathbf{v} \nabla \cdot \mathbf{w} + 2\mu \boldsymbol{\varepsilon}(\mathbf{v}) : \boldsymbol{\varepsilon}(\mathbf{w}) = \boldsymbol{\sigma}(\mathbf{w}) : \nabla \mathbf{v}. \tag{3.11}$$

Substituting this equation into (3.10) and integrating by parts, we can deduce that

$$\begin{aligned} & \int_{\Omega_k} \mathbf{u} \cdot \overline{(\nabla \cdot \boldsymbol{\sigma}(\mathbf{v}) + \omega^2 \rho \mathbf{v})} \, d\mathbf{x} + \int_{\partial\Omega_k} \boldsymbol{\sigma}(\mathbf{u}) \mathbf{n} \cdot \bar{\mathbf{v}} \, dS - \int_{\partial\Omega_k} \mathbf{u} \cdot \overline{\boldsymbol{\sigma}(\mathbf{v})} \, \mathbf{n} \, dS \\ &= \int_{\Omega_k} \mathbf{f} \cdot \bar{\mathbf{v}} \, d\mathbf{x}, \quad \forall \mathbf{v} \in \mathbf{V}(\Omega_k). \end{aligned} \tag{3.12}$$

Using the Trefftz property (3.9) satisfied by the test function  $\mathbf{v}$ , we can obtain the elemental equation defining the PWDG method

$$\int_{\partial\Omega_k} \boldsymbol{\sigma}(\mathbf{u}) \mathbf{n} \cdot \bar{\mathbf{v}} \, dS - \int_{\partial\Omega_k} \mathbf{u} \cdot \overline{\boldsymbol{\sigma}(\mathbf{v})} \, \mathbf{n} \, dS = \int_{\Omega_k} \mathbf{f} \cdot \bar{\mathbf{v}} \, d\mathbf{x}, \quad \forall \mathbf{v} \in \mathbf{V}(\Omega_k). \tag{3.13}$$

Then, the above problem can be discretized as follows: for every  $\Omega_k \in \mathcal{T}_h$ , the vector-valued functions  $\mathbf{u}_h$  satisfy

$$\int_{\partial\Omega_k} \hat{\boldsymbol{\sigma}}(\mathbf{u}_h) \mathbf{n} \cdot \bar{\mathbf{v}}_h \, dS - \int_{\partial\Omega_k} \hat{\mathbf{u}}_h \cdot \overline{\boldsymbol{\sigma}(\mathbf{v}_h)} \, \mathbf{n} \, dS = \int_{\Omega_k} \mathbf{f} \cdot \bar{\mathbf{v}}_h \, d\mathbf{x}, \quad \forall \mathbf{v}_h \in \mathbf{V}_p(\Omega_k). \tag{3.14}$$

where  $\mathbf{V}_p(\Omega_k) \subset \mathbf{V}(\Omega_k)$  is the discretized space to be specified later, and  $\hat{\boldsymbol{\sigma}}(\mathbf{u}_h)$  and  $\hat{\mathbf{u}}_h$  are the single-valued numerical fluxes defined by

$$\begin{cases} \hat{\mathbf{u}}_h = \{\{\mathbf{u}_h\}\} - \beta [[\boldsymbol{\sigma}(\mathbf{u})]], \\ \hat{\boldsymbol{\sigma}}(\mathbf{u}_h) = \{\{\boldsymbol{\sigma}(\mathbf{u}_h)\}\} + \alpha [[\mathbf{u}_h]] \end{cases} \tag{3.15}$$

on  $\mathcal{F}_h^I$ , and

$$\begin{cases} \hat{\mathbf{u}}_h = \mathbf{u}_h - i\delta \eta^{-1} \left( \boldsymbol{\sigma}(\mathbf{u}) \mathbf{n} - i\eta \mathbf{u} - \mathbf{g} \right), \\ \hat{\boldsymbol{\sigma}}(\mathbf{u}_h) = \boldsymbol{\sigma}(\mathbf{u}) - (1 - \delta) \left( \boldsymbol{\sigma}(\mathbf{u}) \mathbf{n} - i\eta \mathbf{u} - \mathbf{g} \right) \otimes \mathbf{n} \end{cases} \tag{3.16}$$

on  $\mathcal{F}_h^B$ , where the parameters  $\alpha$ ,  $\beta$  and  $\delta$  are strictly positive constants, with  $0 < \delta \leq 1/2$ .

Defining the finite-dimensional discretized space

$$\mathbf{V}_p(\mathcal{T}_h) = \{\mathbf{u}_h \in (L^2(\Omega))^d; \mathbf{u}_h \in \mathbf{V}_p(\Omega_k) \text{ on each } \Omega_k\},$$

inserting the numerical fluxes into (3.14) and adding over all elements finish the definition of the PWDG method: find  $\mathbf{u}_h^{(2)} \in \mathbf{V}_p(\mathcal{T}_h)$  such that,

$$\mathcal{A}_h(\mathbf{u}_h^{(2)}, \mathbf{v}_h) = \ell_h(\mathbf{v}_h), \quad \forall \mathbf{v}_h \in \mathbf{V}_p(\mathcal{T}_h), \tag{3.17}$$

where

$$\begin{aligned} \mathcal{A}_h(\mathbf{u}, \mathbf{v}) &= \int_{\mathcal{F}_h^I} \{\{\boldsymbol{\sigma}(\mathbf{u})\}\} \mathbf{n} \cdot \overline{[[\mathbf{v}]]} \, \mathbf{n} \, dS + \int_{\mathcal{F}_h^I} \alpha [[\mathbf{u}]] \mathbf{n} \cdot \overline{[[\mathbf{v}]]} \, \mathbf{n} \, dS \\ &\quad - \int_{\mathcal{F}_h^I} \{\{\mathbf{u}\}\} \cdot \overline{[[\boldsymbol{\sigma}(\mathbf{v})]]} \, dS + \int_{\mathcal{F}_h^I} \beta [[\boldsymbol{\sigma}(\mathbf{u})]] \cdot \overline{[[\boldsymbol{\sigma}(\mathbf{v})]]} \, dS \\ &\quad + \int_{\mathcal{F}_h^B} \delta \boldsymbol{\sigma}(\mathbf{u}) \mathbf{n} \cdot \bar{\mathbf{v}} \, dS + \int_{\mathcal{F}_h^B} \delta \mathbf{u} \cdot \overline{\boldsymbol{\sigma}(\mathbf{v})} \, \mathbf{n} \, dS + \int_{\mathcal{F}_h^B} (1 - \delta) i\eta \mathbf{u} \cdot \bar{\mathbf{v}} \, dS \end{aligned}$$

$$- \int_{\mathcal{F}_h^B} \mathbf{u} \cdot \overline{\boldsymbol{\sigma}(\mathbf{v})} \mathbf{n} \, dS + \int_{\mathcal{F}_h^B} i\delta\eta^{-1} \boldsymbol{\sigma}(\mathbf{u}) \mathbf{n} \cdot \overline{\boldsymbol{\sigma}(\mathbf{v})} \mathbf{n} \, dS, \tag{3.18}$$

and

$$\begin{aligned} \ell_h(\mathbf{v}) &= \sum_k \int_{\Omega_k} \mathbf{f} \cdot \bar{\mathbf{v}} \, d\mathbf{x} - \mathcal{A}_h(\mathbf{u}_h^{(1)}, \mathbf{v}) \\ &\quad - \int_{\mathcal{F}_h^B} (1 - \delta) \mathbf{g} \cdot \bar{\mathbf{v}} \, dS + \int_{\mathcal{F}_h^B} i\delta\eta^{-1} \mathbf{g} \cdot \overline{\boldsymbol{\sigma}(\mathbf{v})} \mathbf{n} \, dS. \end{aligned} \tag{3.19}$$

### 3.3 Auxiliary results

Here, we collect technical prerequisites for the convergence analysis.

Define the broken Sobolev space

$$H^r(\mathcal{T}_h) = \{\mathbf{w} \in L^2(\Omega)^d : \mathbf{w}|_{\Omega_k} \in H^r(\Omega_k)^d, \quad \forall \Omega_k \in \mathcal{T}_h\}. \tag{3.20}$$

Let  $\mathbf{T}(\mathcal{T}_h)$  be the piecewise Trefftz space defined on  $\mathcal{T}_h$  by

$$\begin{aligned} \mathbf{T}(\mathcal{T}_h) &= \left\{ \mathbf{w} \in L^2(\Omega)^d : \exists s > 1/2 \text{ s.t. } \mathbf{w} \in H^{1+s}(\mathcal{T}_h), \right. \\ &\quad \left. \text{and } \nabla \cdot \boldsymbol{\sigma}(\mathbf{w}) + \omega^2 \rho \mathbf{w} = \mathbf{0} \text{ in each } \Omega_k \in \mathcal{T}_h \right\}. \end{aligned} \tag{3.21}$$

We endow  $\mathbf{T}(\mathcal{T}_h)$  with the mesh-skeleton norm

$$\begin{aligned} |||\mathbf{w}|||_{\mathcal{F}_h}^2 &= |||\beta^{1/2}[\boldsymbol{\sigma}(\mathbf{w})]|||_{0, \mathcal{F}_h^I}^2 + |||\alpha^{1/2}[\{\mathbf{w}\}] \mathbf{n}|||_{0, \mathcal{F}_h^I}^2 \\ &\quad + |||\delta^{1/2} \eta^{-1/2} \boldsymbol{\sigma}(\mathbf{w}) \mathbf{n}|||_{0, \mathcal{F}_h^B}^2 + |||(1 - \delta)^{1/2} \eta^{1/2} \mathbf{w}|||_{0, \mathcal{F}_h^B}^2 \end{aligned} \tag{3.22}$$

and the following augmented norm

$$\begin{aligned} |||\mathbf{w}|||_{\mathcal{F}_h^+}^2 &= |||\mathbf{w}|||_{\mathcal{F}_h}^2 + |||\beta^{-1/2}\{\{\mathbf{w}\}\}|||_{0, \mathcal{F}_h^I}^2 \\ &\quad + |||\alpha^{-1/2}\{\{\boldsymbol{\sigma}(\mathbf{w})\}\}|||_{0, \mathcal{F}_h^I}^2 + |||\delta^{-1/2} \eta^{1/2} \mathbf{w}|||_{0, \mathcal{F}_h^B}^2. \end{aligned} \tag{3.23}$$

**Lemma 3.1** *If  $\mathbf{u}, \mathbf{v} \in \mathbf{T}(\mathcal{T}_h)$ , we have*

$$\begin{aligned} \mathcal{A}_h(\mathbf{u}, \mathbf{v}) &= \mathcal{A}_h(\bar{\mathbf{v}}, \bar{\mathbf{u}}), \\ -Im[\mathcal{A}_h(\mathbf{u}, \mathbf{u})] &= |||\mathbf{u}|||_{\mathcal{F}_h}^2, \\ \text{and } |\mathcal{A}_h(\mathbf{u}, \mathbf{v})| &\leq C |||\mathbf{u}|||_{\mathcal{F}_h^+} |||\mathbf{v}|||_{\mathcal{F}_h}. \end{aligned} \tag{3.24}$$

**Proof** Provided that  $\mathbf{u}, \mathbf{v} \in \mathbf{T}(\mathcal{T}_h)$ , local integration by parts permits us to obtain

$$\begin{aligned} 0 &= \sum_{k=1}^N \int_{\Omega_k} \mathbf{u} \cdot (\nabla \cdot \overline{\boldsymbol{\sigma}(\mathbf{v})} + \omega^2 \rho \mathbf{v}) \, d\mathbf{x} \\ &= \sum_{k=1}^N \int_{\Omega_k} -\nabla \mathbf{u} : \overline{\boldsymbol{\sigma}(\mathbf{v})} + \omega^2 \rho \mathbf{u} \cdot \bar{\mathbf{v}} \, d\mathbf{x} + \sum_{k=1}^N \int_{\partial\Omega_k} \mathbf{u} \cdot \overline{\boldsymbol{\sigma}(\mathbf{v})} \mathbf{n} \, dS. \end{aligned} \tag{3.25}$$



By the direct calculation, we can obtain

$$\sum_{k=1}^N \int_{\partial\Omega_k} \mathbf{u} \cdot \overline{\boldsymbol{\sigma}(\mathbf{v})} \mathbf{n} \, dS = \int_{\mathcal{F}_h^B} \mathbf{u} \cdot \overline{\boldsymbol{\sigma}(\mathbf{v})} \mathbf{n} \, dS + \int_{\mathcal{F}_h^I} \{\{\mathbf{u}\}\} \cdot \overline{[\boldsymbol{\sigma}(\mathbf{v})]} + [[\mathbf{u}]] \mathbf{n} \overline{\{\{\boldsymbol{\sigma}(\mathbf{v})\}\}} \mathbf{n} \, dS. \tag{3.26}$$

Substituting (3.11) and (3.26) into (3.25), we have

$$0 = \sum_{k=1}^N \int_{\Omega_k} -\lambda \nabla \cdot \mathbf{u} \overline{\nabla \cdot \mathbf{v}} - 2\mu \boldsymbol{\varepsilon}(\mathbf{u}) : \overline{\boldsymbol{\varepsilon}(\mathbf{v})} + \omega^2 \rho \mathbf{u} \cdot \overline{\mathbf{v}} \, dx + \int_{\mathcal{F}_h^B} \mathbf{u} \cdot \overline{\boldsymbol{\sigma}(\mathbf{v})} \mathbf{n} \, dS + \int_{\mathcal{F}_h^I} \{\{\mathbf{u}\}\} \cdot \overline{[\boldsymbol{\sigma}(\mathbf{v})]} + [[\mathbf{u}]] \mathbf{n} \overline{\{\{\boldsymbol{\sigma}(\mathbf{v})\}\}} \mathbf{n} \, dS. \tag{3.27}$$

Adding (3.27) to (3.18) gives

$$\begin{aligned} \mathcal{A}_h(\mathbf{u}, \mathbf{v}) = & \sum_{k=1}^N \int_{\Omega_k} -\lambda \nabla \cdot \mathbf{u} \overline{\nabla \cdot \mathbf{v}} - 2\mu \boldsymbol{\varepsilon}(\mathbf{u}) : \overline{\boldsymbol{\varepsilon}(\mathbf{v})} + \omega^2 \rho \mathbf{u} \cdot \overline{\mathbf{v}} \, dx \\ & + \int_{\mathcal{F}_h^I} \{\{\boldsymbol{\sigma}(\mathbf{u})\}\} \mathbf{n} \cdot \overline{[[\mathbf{v}]] \mathbf{n}} \, dS + \int_{\mathcal{F}_h^I} [[[\mathbf{u}]]] \mathbf{n} \cdot \overline{\{\{\boldsymbol{\sigma}(\mathbf{v})\}\}} \mathbf{n} \, dS \\ & + \int_{\mathcal{F}_h^B} \delta \boldsymbol{\sigma}(\mathbf{u}) \mathbf{n} \cdot \overline{\mathbf{v}} \, dS + \int_{\mathcal{F}_h^B} \delta \mathbf{u} \cdot \overline{\boldsymbol{\sigma}(\mathbf{v})} \mathbf{n} \, dS \\ & + \int_{\mathcal{F}_h^I} \alpha [[[\mathbf{u}]]] \mathbf{n} \cdot \overline{[[\mathbf{v}]] \mathbf{n}} \, dS + \int_{\mathcal{F}_h^I} \beta [\boldsymbol{\sigma}(\mathbf{u})] \cdot \overline{[\boldsymbol{\sigma}(\mathbf{v})]} \, dS \\ & + \int_{\mathcal{F}_h^B} (1 - \delta) i \eta \mathbf{u} \cdot \overline{\mathbf{v}} \, dS + \int_{\mathcal{F}_h^B} i \delta \eta^{-1} \boldsymbol{\sigma}(\mathbf{u}) \mathbf{n} \cdot \overline{\boldsymbol{\sigma}(\mathbf{v})} \mathbf{n} \, dS. \end{aligned} \tag{3.28}$$

Therefore, we can directly obtain the first equality of (3.24).

By taking the imaginary part of (3.28), we get the second equality of (3.24).

By the definition of  $\mathcal{A}_h(\cdot, \cdot)$ ,  $\delta^{\frac{1}{2}} \leq (1 - \delta)^{\frac{1}{2}}$  and repeated applications of the weighted Cauchy–Schwarz inequality, we can deduce the third inequality of (3.24).  $\square$

## 4 Discretization of the variational problems

In this section, we introduce discretizations of the variational problems described in the last section.

### 4.1 Spectral element discretization of the local nonhomogeneous problems

Since  $\Omega_k^*$  is a sufficiently smooth domain and  $\mathbf{f}$  is smooth on  $\Omega_k^*$ , the solution  $\mathbf{u}_k^{(1)}$  possesses high regularity on  $\Omega_k^*$ . Moreover, the fictitious domain  $\Omega_k^*$  has almost the same size as the element  $\Omega_k$ . Thus, the subproblems (3.3) should be discretized by the spectral element method, so that the resulting approximate solutions have higher accuracies.

Let  $q$  be a positive integer and  $D$  be a bounded and connected domain in  $\mathbb{R}^d$ . Let  $S_q(D)$  denote the set of polynomials defined on  $D$ , whose orders are less than or equal to  $q$ . Set  $\mathbf{S}_q(D) = (S_q(D))^d$ .

The discrete variational problems of Eq. (3.3) are: to find  $\mathbf{u}_{k,h}^{(1)} \in \mathbf{S}_q(\Omega_k^*)$  such that

$$\left\{ \begin{aligned} & \int_{\Omega_k^*} (-\lambda \nabla \cdot \mathbf{u}_{k,h}^{(1)} \overline{\nabla \cdot \mathbf{v}_{k,h}} - 2\mu \varepsilon(\mathbf{u}_{k,h}^{(1)}) \cdot \overline{\varepsilon(\mathbf{v}_{k,h})} + \omega^2 \rho \mathbf{u}_{k,h}^{(1)} \cdot \overline{\mathbf{v}_{k,h}}) \, d\mathbf{x} \\ & + \int_{\partial\Omega_k^*} i \eta \mathbf{u}_{k,h}^{(1)} \cdot \overline{\mathbf{v}_{k,h}} \, dS \\ & = \int_{\Omega_k^*} \mathbf{f} \cdot \overline{\mathbf{v}_{k,h}} \, d\mathbf{x}, \quad \forall \mathbf{v}_{k,h} \in \mathbf{S}_q(\Omega_k^*) \quad (k = 1, 2, \dots, N). \end{aligned} \right. \tag{4.1}$$

In this paper, we choose the fictitious domain  $\Omega_k^*$  to be a disc for the two-dimensional case or a sphere for the three-dimensional case (see Remark 2.1 in Hu and Yuan (2018)). Then, the variational problems (4.1) can be solved easily using the polar coordinate transformation for the calculation of the involved integrations. We would like to emphasize that the discrete problems (4.1) are local and independent each other for  $k = 1, \dots, N$ , so they can be solved in parallel and the cost is very small.

Define  $\mathbf{u}_h^{(1)} \in \prod_{k=1}^N \mathbf{S}_q(\Omega_k)$  by  $\mathbf{u}_h^{(1)}|_{\Omega_k} = \mathbf{u}_{k,h}^{(1)}|_{\Omega_k}$ .

### 4.2 Basis functions of $\mathbf{V}_p(\mathcal{T}_h)$

In this section, we describe the discretization of the variational problem (3.17). The discretization is based on a finite-dimensional space  $\mathbf{V}_p(\mathcal{T}_h) \subset \mathbf{V}(\mathcal{T}_h)$ . We first give the precise definition of such a space  $\mathbf{V}_p(\mathcal{T}_h)$ .

Let us consider a time-harmonic elastic plane wave moving in an unit direction  $\mathbf{d}$ . The plane wave can be split into two components for two-dimensional case:

$$\mathbf{v} = x_P \mathbf{d} \exp(i\kappa_P \mathbf{d} \cdot \mathbf{x}) + y_S \mathbf{e} \exp(i\kappa_S \mathbf{d} \cdot \mathbf{x}) \tag{4.2}$$

and three components for three-dimensional case:

$$\mathbf{v} = x_P \mathbf{d} \exp(i\kappa_P \mathbf{d} \cdot \mathbf{x}) + y_S \mathbf{e} \exp(i\kappa_S \mathbf{d} \cdot \mathbf{x}) + z_S \mathbf{f} \exp(i\kappa_S \mathbf{d} \cdot \mathbf{x}), \tag{4.3}$$

where the wavenumbers  $\kappa_P = \omega/C_P$  and  $\kappa_S = \omega/C_S$ ,  $x_P$ ,  $y_S$  and  $z_S$  are scalar coefficients, and  $\mathbf{d} \cdot \mathbf{e} = 0$ ,  $\mathbf{f} = \mathbf{e} \times \mathbf{d}$ . The first component, denoted by  $\mathbf{v}_P = x_P \mathbf{d} \exp(i\kappa_P \mathbf{d} \cdot \mathbf{x})$ , is called the compressional ( $P$ -) wave, and we see that  $\nabla \times \mathbf{v}_P = \mathbf{0}$  and that  $\mathbf{v}_P$  is a solution of the Navier equation by the definition of the wavenumber  $\kappa_P$  and the wave speed  $C_P$  for the  $P$ -wave.

Similarly, the remaining components of the plane wave solution, called the shear ( $S$ -) wave and given by  $\mathbf{v}_S = y_S \mathbf{e} \exp(i\kappa_S \mathbf{d} \cdot \mathbf{x}) \left( + z_S \mathbf{f} \exp(i\kappa_S \mathbf{d} \cdot \mathbf{x}) \text{ for three-dimensional case} \right)$ , are a solution of the Navier equation by the definition of the wavenumber  $\kappa_S$  and the wave speed  $C_S$  for the  $S$ -wave. Moreover, in this case,  $\nabla \cdot \mathbf{v}_S = 0$ .

In a homogeneous medium, the  $P$ -wave  $\mathbf{v}_P$  and  $S$ -wave  $\mathbf{v}_S$  satisfy the Helmholtz equations

$$\begin{cases} \Delta \mathbf{v}_P + \kappa_P^2 \mathbf{v}_P = \mathbf{0} \\ \Delta \mathbf{v}_S + \kappa_S^2 \mathbf{v}_S = \mathbf{0}. \end{cases} \quad \text{in } \Omega_k. \tag{4.4}$$

These two component waves propagate independently in the homogeneous medium but interact on the medium interfaces.

In practice, a suitable family of plane waves, which are solutions of the constant-coefficient Helmholtz equations, is generated on  $\Omega_k$  by choosing  $p$  unit propagation directions  $\mathbf{d}_l$  ( $l = 1, \dots, p$ ). As advocated in earlier studies with the Helmholtz equations (Moiola et al. 2011), the directions  $\mathbf{d}_l$  ( $l = 1, \dots, p$ ) of the wave vectors of these wave functions, for two-dimensional problems, are uniformly distributed by

$$\mathbf{d}_l = \begin{pmatrix} \cos(2\pi(l-1)/p) \\ \sin(2\pi(l-1)/p) \end{pmatrix} \quad (l = 1, \dots, p),$$

and for three-dimensional problems, are generated by the optimal spherical codes from Sloane (2000). We then define two sets of complex plane wave basis functions by setting

$$\begin{cases} \mathbf{v}_l^P = \mathbf{d}_l \exp(i\kappa_P \mathbf{d}_l \cdot \mathbf{x}) \\ \mathbf{v}_l^S = \mathbf{e}_l \exp(i\kappa_S \mathbf{d}_l \cdot \mathbf{x}) \end{cases} \quad (l = 1, \dots, p), \tag{4.5}$$

for two-dimensional case, and three sets of complex plane wave basis functions by setting

$$\begin{cases} \mathbf{v}_l^P = \mathbf{d}_l \exp(i\kappa_P \mathbf{d}_l \cdot \mathbf{x}) \\ \mathbf{v}_{1,l}^S = \mathbf{e}_l \exp(i\kappa_S \mathbf{d}_l \cdot \mathbf{x}) \\ \mathbf{v}_{2,l}^S = \mathbf{f}_l \exp(i\kappa_S \mathbf{d}_l \cdot \mathbf{x}) \end{cases} \quad (l = 1, \dots, p), \tag{4.6}$$

for three-dimensional case.

Let  $\mathcal{Q}_t$  ( $t = 2p$  for two-dimensional case and  $t = 3p$  for three-dimensional case) denote the space spanned by the  $t$  plane wave functions. Define the finite-element space

$$\mathbf{V}_p(\mathcal{T}_h) = \left\{ \mathbf{v} \in (H^1(\Omega))^d : \mathbf{v}|_K \in \mathcal{Q}_t \text{ for any } K \in \mathcal{T}_h \right\}. \tag{4.7}$$

It is easy to see that the above space has  $N \times t$  basis functions, which are defined by

$$\mathbf{v}_{k,l}^P(\mathbf{x}) = \begin{cases} \mathbf{v}_l^P(\mathbf{x}), & \mathbf{x} \in \Omega_k, \\ 0, & \mathbf{x} \in \Omega_j \text{ satisfying } j \neq k \end{cases} \quad (k = 1, \dots, N; l = 1, \dots, p), \tag{4.8}$$

and

$$\mathbf{v}_{k,l}^S(\mathbf{x}) = \begin{cases} \mathbf{v}_l^S(\mathbf{x}), & \mathbf{x} \in \Omega_k, \\ 0, & \mathbf{x} \in \Omega_j \text{ satisfying } j \neq k \end{cases} \quad (k = 1, \dots, N; l = 1, \dots, p) \tag{4.9}$$

for two-dimensional case, and by  $\mathbf{v}_{k,l}^P$  defined in Eq. (4.8) and  $\mathbf{v}_{k,l}^S$  defined in Eq. (4.10) for three-dimensional case, where

$$\mathbf{v}_{k,s,l}^S(\mathbf{x}) = \begin{cases} \mathbf{v}_{s,l}^S(\mathbf{x}), & \mathbf{x} \in \Omega_k, \\ 0, & \mathbf{x} \in \Omega_j \text{ satisfying } j \neq k \end{cases} \quad (k = 1, \dots, N; s = 1, 2; l = 1, \dots, p). \tag{4.10}$$

For simplicity of claim in the section of error analysis, we decompose the finite-element space  $\mathbf{V}_p(\mathcal{T}_h)$  into two components by

$$\mathbf{V}_p(\mathcal{T}_h) = \mathbf{V}_p^S(\mathcal{T}_h) + \mathbf{V}_p^P(\mathcal{T}_h), \tag{4.11}$$

where the space  $\mathbf{V}_p^S(\mathcal{T}_h)$  is spanned by plane wave basis functions  $\mathbf{v}_{k,l}^S$  for two-dimensional case or  $\mathbf{v}_{k,s,l}^S$  for three-dimensional case, and the space  $\mathbf{V}_p^P(\mathcal{T}_h)$  is spanned by plane wave basis functions  $\mathbf{v}_{k,l}^P$ .

We can now define an approximation  $\mathbf{u}_h^{(2)}$  of  $\mathbf{u}^{(2)}$  by

$$\mathbf{u}_h^{(2)}|_{\Omega_k} = \mathbf{u}_{k,h}^{(2)} = \sum_{l=1}^P x_{k,l} \mathbf{v}_{k,l}^P + \sum_{l=1}^P y_{k,l} \mathbf{v}_{k,l}^S \doteq \mathbf{u}_{k,h}^P + \mathbf{u}_{k,h}^S \tag{4.12}$$

for two-dimensional case, and

$$\mathbf{u}_h^{(2)}|_{\Omega_k} = \mathbf{u}_{k,h}^{(2)} = \sum_{l=1}^P x_{k,l} \mathbf{v}_{k,l}^P + \sum_{l=1}^P (y_{k,l} \mathbf{v}_{k,1,l}^S + z_{k,l} \mathbf{v}_{k,2,l}^S) \doteq \mathbf{u}_{k,h}^P + \mathbf{u}_{k,h}^S \tag{4.13}$$

for three-dimensional case.

Define  $\mathbf{u}_h^P$  by  $\mathbf{u}_h^P|_{\Omega_k} = \mathbf{u}_{k,h}^P$ ,  $\mathbf{u}_h^S$  by  $\mathbf{u}_h^S|_{\Omega_k} = \mathbf{u}_{k,h}^S$  and  $\mathbf{u}_h^{(2)} = \mathbf{u}_h^P + \mathbf{u}_h^S$ .

### 5 Error estimates of the elastic PWDG–LSFE method

In this section, we derive the error estimates of the approximate solutions  $\mathbf{u}_h$  defined in the previous section. We mention that the proofs of error estimates of the approximate solutions generated by the proposed method are a translation to the elastic wave case of techniques already used for acoustic and electromagnetic waves (see Hu and Yuan 2018). Besides, we directly use the sharp approximation estimate (see Lemma 5.3) of homogeneous elastic wave equations by plane wave basis functions, which was first introduced by Moiola in (Moiola 2013, Theorem 3.2). Moreover, we underline that the proof of Lemma 5.5 is based on the technique of Theorem 3.13 from [25].

Assume a domain  $D \subset \Omega$ . Let  $\|\cdot\|_{s,\omega,D}$  be the  $\omega$ -weighted Sobolev norm defined by

$$\|v\|_{s,\omega,D}^2 = \sum_{j=0}^s \omega^{2(s-j)} |v|_{j,D}^2.$$

In the rest of this paper, we always use  $C$  to denote a generic positive constant independent of  $h$ ,  $p$  and  $\omega$ , but its value might change at different occurrence. Moreover, we assume that each  $\Omega_k^*$  is a disc or a sphere, whose radius and center are denoted by  $r_k$  and  $O_k$ , respectively.

#### 5.1 Error estimate of the local spectral element approximations

In this section, we derive the error estimates of the approximate solutions  $\mathbf{u}_h^{(1)}$  based on the framework introduced in Hu and Yuan (2018).

We first give a stability result of  $\mathbf{u}_k^{(1)}$  for each  $k$ .

**Lemma 5.1** *Assume that  $c_0 \leq h\omega \leq C_0$  and  $\mathbf{f} \in \mathbf{H}^{r-1}(\Omega_k^*)$  with an integer  $r \geq 1$ . Let  $\mathbf{u}_k^{(1)}$  denote the solution of the nonhomogeneous local equation (3.2). Then,  $\mathbf{u}_k^{(1)} \in \mathbf{H}^{r+1}(\Omega_k^*)$  and*

$$|\mathbf{u}_k^{(1)}|_{r+1,\Omega_k^*} \leq C \sum_{l=0}^{r-1} \omega^{r-1-l} \|\mathbf{f}\|_{l,\Omega_k^*}. \tag{5.1}$$

**Proof** Define the scaling transformation  $\hat{\mathbf{x}} = F_k(\mathbf{x}) = r_k^{-1}(\mathbf{x} - O_k) + O_k$ . Under the coordinate transformation  $\hat{\mathbf{x}} = F_k(\mathbf{x})$ , set  $\mathbf{u}_k^{(1)}(\mathbf{x}) = \mathbf{u}_k^{(1)}(F_k^{-1}(\hat{\mathbf{x}})) = \hat{\mathbf{u}}_k^{(1)}(\hat{\mathbf{x}})$ . Besides,  $\Omega_k^*$  is

mapped to a disc ( $2d$  case) or a sphere ( $3d$  case) with the radius one, which is denoted by  $\hat{D}_k$ . Set  $\hat{\omega}_k = r_k \omega$ . Then, the equation (3.2) becomes

$$\begin{cases} \mu \hat{\Delta} \hat{\mathbf{u}}_k^{(1)} + (\lambda + \mu) \hat{\nabla} (\hat{\nabla} \cdot \hat{\mathbf{u}}_k^{(1)}) + \hat{\omega}^2 \rho \hat{\mathbf{u}}_k^{(1)} = r_k^2 \hat{\mathbf{f}} & \text{in } \hat{D}_k \\ \hat{\mathbf{T}}^{(\mathbf{n}_k)}(\hat{\mathbf{u}}_k^{(1)}) - i \hat{\eta} \hat{\mathbf{u}}_k^{(1)} = 0 & \text{on } \partial \hat{D}_k. \end{cases} \tag{5.2}$$

By the smoothness assumption of  $\mathbf{f}$ ,  $\hat{\omega}_k = O(1)$  and the existing regularity results (see, for example, Theorem 2 in Cummings and Feng (2006) and Lemma 3.3 in Du and Wu (2015)), we know that  $\hat{\mathbf{u}}_k^{(1)} \in H^{r+1}(\hat{D}_k)$  and

$$|\hat{\mathbf{u}}_k^{(1)}|_{r+1, \hat{D}_k} \leq C \sum_{l=0}^{r-1} \hat{\omega}_k^{r-l} \|r_k^2 \hat{\mathbf{f}}\|_{l, \hat{D}_k}. \tag{5.3}$$

Now we use the integral transformation  $\hat{\mathbf{x}} = F_k(\mathbf{x})$  to (5.3), and get the desired results.  $\square$

**Remark 5.1** We point out that it is unclear whether the assumption  $\omega h \geq c_0$  is indeed necessary for the estimate (5.1). Besides, at least in the case with nonsingular solutions, for the plane wave method and the spectral element method for the considered equations, increasing the number  $p$  of basis functions on every element is more efficient than decreasing the mesh size  $h$  to get approximate solutions with high accuracy. From the viewpoint of the numerical results for the case of smooth solutions, we can simply choose  $h \approx \frac{1}{\omega}$ . Thus, the assumption  $\omega h \geq c_0$  is not a limit in applications with smooth solutions. In future work, we will give detailed numerical analysis of our method for the case of non-smooth analytic solution.

The following result gives estimates of the local spectral element approximations  $\mathbf{u}_{k,h}^{(1)}$  ( $k = 1, \dots, N$ ).

**Lemma 5.2** *Let  $q \geq 2$  and  $2 \leq r + 1 \leq q + 1$ . Under the assumptions in Lemma 5.1, we have for each  $\Omega_k^*$*

$$\|\mathbf{u}_k^{(1)} - \mathbf{u}_{k,h}^{(1)}\|_{j, \Omega_k^*} \leq C \left(\frac{h}{q}\right)^{r+1-j} |\mathbf{u}_k^{(1)}|_{r+1, \Omega_k^*} \quad (j = 0, 1, 2). \tag{5.4}$$

**Proof** We use the same notations with that in the proof of the above Lemma. Under the scaling transformation  $\hat{\mathbf{x}} = F_k(\mathbf{x})$ , the variational problems (3.3) and (3.3) become

$$\begin{cases} \int_{\hat{D}_k} (-\lambda \nabla \cdot \hat{\mathbf{u}}_k^{(1)} \overline{\nabla \cdot \mathbf{v}_k} - 2\mu \varepsilon(\hat{\mathbf{u}}_k^{(1)}) \cdot \overline{\varepsilon(\mathbf{v}_k)} + \hat{\omega}_k^2 \rho \hat{\mathbf{u}}_k^{(1)} \cdot \overline{\mathbf{v}_k}) d\hat{\mathbf{x}} + \int_{\partial \hat{D}_k} i \hat{\eta} \hat{\mathbf{u}}_k^{(1)} \cdot \overline{\mathbf{v}_k} dS \\ = \int_{\hat{D}_k} r_k^2 \hat{\mathbf{f}} \cdot \overline{\mathbf{v}_k} d\hat{\mathbf{x}}, \quad \forall \mathbf{v}_k \in \mathbf{H}^1(\hat{D}_k) \quad (k = 1, 2, \dots, N), \end{cases} \tag{5.5}$$

and

$$\begin{cases} \int_{\hat{D}_k} (-\lambda \nabla \cdot \hat{\mathbf{u}}_{k,h}^{(1)} \overline{\nabla \cdot \mathbf{v}_k} - 2\mu \varepsilon(\hat{\mathbf{u}}_{k,h}^{(1)}) \cdot \overline{\varepsilon(\mathbf{v}_k)} + \hat{\omega}_k^2 \rho \hat{\mathbf{u}}_{k,h}^{(1)} \cdot \overline{\mathbf{v}_k}) d\hat{\mathbf{x}} + \int_{\partial \hat{D}_k} i \hat{\eta} \hat{\mathbf{u}}_{k,h}^{(1)} \cdot \overline{\mathbf{v}_k} dS \\ = \int_{\hat{D}_k} r_k^2 \hat{\mathbf{f}} \cdot \overline{\mathbf{v}_k} d\hat{\mathbf{x}}, \quad \forall \mathbf{v}_k \in \mathbf{S}_q(\hat{D}_k) \quad (k = 1, 2, \dots, N), \end{cases} \tag{5.6}$$

respectively. We first derive an error estimate of  $\hat{\mathbf{u}}_k^{(1)} - \hat{\mathbf{u}}_{k,h}^{(1)}$  based on the framework introduced in Feng and Wu (2011). Let  $\hat{\mathbf{P}}_q : \mathbf{H}^1(\hat{D}_k) \rightarrow \mathbf{S}_q(\hat{D}_k)$  denote the orthogonal projector

associated with the complex inner product

$$\int_{\hat{D}_k} (-\lambda \nabla \cdot \hat{\mathbf{v}} \overline{\nabla \cdot \mathbf{w}} - 2\mu \varepsilon(\hat{\mathbf{v}}) \cdot \overline{\varepsilon(\mathbf{w})}) d\hat{\mathbf{x}} + \int_{\partial \hat{D}_k} i \hat{\eta} \hat{\mathbf{v}} \cdot \overline{\mathbf{w}} dS, \quad \mathbf{v}, \mathbf{w} \in \mathbf{H}^1(\hat{D}_k).$$

Then,  $\hat{\mathbf{P}}_q \hat{\mathbf{u}}_k^{(1)}$  satisfies

$$\begin{aligned} & \int_{\hat{D}_k} \left( -\lambda \nabla \cdot (\hat{\mathbf{P}}_q \hat{\mathbf{u}}_k^{(1)}) \overline{\nabla \cdot \mathbf{w}} - 2\mu \varepsilon(\hat{\mathbf{P}}_q \hat{\mathbf{u}}_k^{(1)}) \cdot \overline{\varepsilon(\mathbf{w})} \right) d\hat{\mathbf{x}} + \int_{\partial \hat{D}_k} i \hat{\eta} (\hat{\mathbf{P}}_q \hat{\mathbf{u}}_k^{(1)}) \cdot \overline{\mathbf{w}} dS \\ &= \int_{\hat{D}_k} (-\lambda \nabla \cdot \hat{\mathbf{u}}_k^{(1)} \overline{\nabla \cdot \mathbf{w}} - 2\mu \varepsilon(\hat{\mathbf{u}}_k^{(1)}) \cdot \overline{\varepsilon(\mathbf{w})}) d\hat{\mathbf{x}} \\ &+ \int_{\partial \hat{D}_k} i \hat{\eta} \hat{\mathbf{u}}_k^{(1)} \cdot \overline{\mathbf{w}} dS, \quad \forall \mathbf{w} \in \mathbf{S}_q(\hat{D}_k). \end{aligned} \tag{5.7}$$

By the approximation of the spectral element method (see, for example, Guo (2007)), there is function  $\hat{\mathbf{v}}_q \in \mathbf{S}_q(\hat{D}_k)$  such that

$$\|\hat{\mathbf{u}}_k^{(1)} - \hat{\mathbf{v}}_q\|_{j, \hat{D}_k} \leq Cq^{-(r+1-j)} |\hat{\mathbf{u}}_k^{(1)}|_{r+1, \hat{D}_k} \quad (j = 0, 1, 2). \tag{5.8}$$

Then, by the standard technique (Zhu and Wu 2013, Sec 3.3), we can show that

$$\|\hat{\mathbf{P}}_q \hat{\mathbf{u}}_k^{(1)} - \hat{\mathbf{u}}_k^{(1)}\|_{j, \hat{D}_k} \leq \|\hat{\mathbf{v}}_q - \hat{\mathbf{u}}_k^{(1)}\|_{j, \hat{D}_k} \leq Cq^{-(r+1-j)} |\hat{\mathbf{u}}_k^{(1)}|_{r+1, \hat{D}_k} \quad (j = 0, 1). \tag{5.9}$$

Set  $\boldsymbol{\xi} = \hat{\mathbf{P}}_q \hat{\mathbf{u}}_k^{(1)} - \hat{\mathbf{u}}_k^{(1)}$  and  $\boldsymbol{\zeta} = \hat{\mathbf{u}}_k^{(1)} - \hat{\mathbf{P}}_q \hat{\mathbf{u}}_k^{(1)}$ . Combining (5.6) with (5.7), we know that the function  $\boldsymbol{\zeta} \in \mathbf{S}_q(\hat{D}_k)$  is the solution of the following variational problem (see Feng and Wu 2011)

$$\begin{cases} \int_{\hat{D}_k} (-\lambda \nabla \cdot \boldsymbol{\zeta} \overline{\nabla \cdot \mathbf{v}_k} - 2\mu \varepsilon(\boldsymbol{\zeta}) \cdot \overline{\varepsilon(\mathbf{v}_k)} + \hat{\omega}_k^2 \rho \boldsymbol{\zeta} \cdot \overline{\mathbf{v}_k}) d\hat{\mathbf{x}} + \int_{\partial \hat{D}_k} i \hat{\eta} \boldsymbol{\zeta} \cdot \overline{\mathbf{v}_k} dS \\ = - \int_{\hat{D}_k} \hat{\omega}_k^2 \rho \boldsymbol{\xi} \cdot \overline{\mathbf{v}_k} d\hat{\mathbf{x}}, \quad \forall \mathbf{v}_k \in \mathbf{S}_q(\hat{D}_k). \end{cases} \tag{5.10}$$

Thus, by the stability result given in Theorem 2 of Cummings and Feng (2006), we have

$$\|\boldsymbol{\zeta}\|_{1, \hat{D}_k} \leq C \|\boldsymbol{\xi}\|_{0, \hat{D}_k}.$$

This, together with (5.9), leads to

$$\|\boldsymbol{\zeta}\|_{1, \hat{D}_k} \leq Cq^{-r-1} \|\hat{\mathbf{u}}_k^{(1)}\|_{r+1, \hat{D}_k}.$$

Notice that

$$\hat{\mathbf{u}}_k^{(1)} - \hat{\mathbf{u}}_{k,h}^{(1)} = (\hat{\mathbf{u}}_k^{(1)} - \hat{\mathbf{P}}_q \hat{\mathbf{u}}_k^{(1)}) + (\hat{\mathbf{P}}_q \hat{\mathbf{u}}_k^{(1)} - \hat{\mathbf{u}}_{k,h}^{(1)}).$$

Using (5.9) again, we further get

$$\|\hat{\mathbf{u}}_k^{(1)} - \hat{\mathbf{u}}_{k,h}^{(1)}\|_{j, \hat{D}_k} \leq Cq^{-(r+1-j)} |\hat{\mathbf{u}}_k^{(1)}|_{r+1, \hat{D}_k} \quad (j = 0, 1). \tag{5.11}$$

Making the integral transformation  $\hat{\mathbf{x}} = F_k(\mathbf{x})$  to (5.11), we can deduce that

$$\|\mathbf{u}_k^{(1)} - \mathbf{u}_{k,h}^{(1)}\|_{j, \Omega_k^*} \leq Ch^{r+1-j} q^{-(r+1-j)} |\mathbf{u}_k^{(1)}|_{r+1, \Omega_k^*} \quad (j = 0, 1). \tag{5.12}$$

On the other hand, it follows by (5.8) that

$$\|\mathbf{u}_k^{(1)} - \mathbf{v}_q\|_{j, \Omega_k^*} \leq Ch^{r+1-j} q^{-(r+1-j)} |\mathbf{u}_k^{(1)}|_{r+1, \Omega_k^*} \quad (j = 1, 2). \tag{5.13}$$

By the triangle inequality, we have

$$\|\mathbf{u}_k^{(1)} - \mathbf{u}_{k,h}^{(1)}\|_{2, \Omega_k^*} \leq \|\mathbf{u}_k^{(1)} - \mathbf{v}_q\|_{2, \Omega_k^*} + \|\mathbf{v}_q - \mathbf{u}_{k,h}^{(1)}\|_{2, \Omega_k^*}. \tag{5.14}$$

Applying the inverse estimate to the second term in the right side of the above inequality leads to

$$\begin{aligned} \|\mathbf{v}_q - \mathbf{u}_{k,h}^{(1)}\|_{2,\Omega_k^*} &\leq Cqh^{-1}\|\mathbf{v}_q - \mathbf{u}_{k,h}^{(1)}\|_{1,\Omega_k^*} \\ &= Cqh^{-1}(\|\mathbf{u}_k^{(1)} - \mathbf{v}_q\|_{1,\Omega_k^*} + \|\mathbf{u}_k^{(1)} - \mathbf{u}_{k,h}^{(1)}\|_{1,\Omega_k^*}). \end{aligned}$$

Substituting this into (5.14), and using (5.13) and (5.12), yields

$$\|\mathbf{u}_k^{(1)} - \mathbf{u}_{k,h}^{(1)}\|_{2,\Omega_k^*} \leq Ch^{r+1-2}q^{-(r+1-2)}|\mathbf{u}_k^{(1)}|_{r+1,\Omega_k^*}.$$

This, together with (5.12), gives the desired result (5.4). □

Combining Lemma 5.1 with Lemma 5.4, using the trace inequality and the definition of the norm  $\|\cdot\|_{\mathcal{F}_h}$  and  $\|\cdot\|_{\mathcal{F}_h^+}$ , we can derive error estimates of the approximation  $\mathbf{u}_h^{(1)}$  easily, and we will omit the details and only give the main results.

**Theorem 5.1** *Let  $q \geq 2$  and  $2 \leq r + 1 \leq q + 1$ . Assume that  $c_0 \leq h\omega \leq C_0$  and  $f \in \mathbf{H}^{r-1}(\Omega_{\tilde{\delta}})$ . Then, the following error estimates hold*

$$\left( \sum_{k=1}^N \|\mathbf{u}^{(1)} - \mathbf{u}_h^{(1)}\|_{j,\Omega_k}^2 \right)^{\frac{1}{2}} \leq C \left(\frac{h}{q}\right)^{r+1-j} \sum_{l=0}^{r-1} \omega^{r-1-l} \|f\|_{l,\Omega_{\tilde{\delta}}} \quad (j = 0, 1, 2) \quad (5.15)$$

and

$$\|\|\mathbf{u}^{(1)} - \mathbf{u}_h^{(1)}\|\|_{\mathcal{F}_h}, \|\|\mathbf{u}^{(1)} - \mathbf{u}_h^{(1)}\|\|_{\mathcal{F}_h^+} \leq C \left(\frac{h}{q}\right)^{r-\frac{1}{2}} \sum_{l=0}^{r-1} \omega^{r-1-l} \|f\|_{l,\Omega_{\tilde{\delta}}}, \quad (5.16)$$

where  $\Omega_{\tilde{\delta}}$  (see (Hu and Yuan 2018, Sec. 4.1.1) ) is the union of  $\Omega$  and the boundary layer with the thickness  $\tilde{\delta} > 0$ .

### 5.2 Error estimate of the plane wave approximations for three-dimensional case

The method of analysis for the electromagnetic PWLS presented in Hu and Yuan (2014b) applies to the elastic PWDG method with major changes in the derivation of the variational formulations and the approximation properties of the elastic plane wave basis functions. We directly use the sharp approximation estimate (see Lemma 5.3) of homogeneous elastic wave equations by plane wave basis functions, which was first introduced by Moiola in (Moiola 2013, Theorem 3.2).

It is known that under the constitutive relation, Eq. (3.4) can be rewritten as the following equation:

$$\mathbf{u}^{(2)} + \frac{1}{\kappa_P^2} \nabla(\nabla \cdot \mathbf{u}^{(2)}) - \frac{1}{\kappa_S^2} \nabla \times (\nabla \times \mathbf{u}^{(2)}) = 0 \quad \text{in } \Omega. \quad (5.17)$$

Let  $\mathbf{u}^P = -\frac{1}{\kappa_P^2} \nabla(\nabla \cdot \mathbf{u}^{(2)})$  be the compressional part ( $P$ - wave) and  $\mathbf{u}^S = \frac{1}{\kappa_S^2} \nabla \times (\nabla \times \mathbf{u}^{(2)})$  be the shear part ( $S$ - wave) of the wave field. Then, we have  $\mathbf{u}^{(2)} = \mathbf{u}^P + \mathbf{u}^S$  in  $\Omega$ ,  $\nabla \times \mathbf{u}^P = \mathbf{0}$  and  $\nabla \cdot \mathbf{u}^S = 0$  in  $\Omega$ . It is easy to verify that  $\mathbf{u}^P$  and  $\mathbf{u}^S$  satisfy the homogeneous vector Helmholtz equations

$$\begin{cases} \Delta \mathbf{u}^P + \kappa_P^2 \mathbf{u}^P = \mathbf{0} \\ \Delta \mathbf{u}^S + \kappa_S^2 \mathbf{u}^S = \mathbf{0}. \end{cases} \quad \text{in } \Omega. \quad (5.18)$$

Let the mesh triangulation  $\mathcal{T}_h$  satisfies the definition stated in (Hiptmair et al. 2013, Section 5) and set  $\tau = \min_{K \in \mathcal{T}_h} \tau_K$ , where  $\tau_K$  is the positive parameter that depends only on the shape of an element  $K$  of  $\mathcal{T}_h$  introduced in (Moiola et al. 2011, Theorem 3.2). Let  $r$  and  $m$  be given positive integers satisfying  $m \geq 2r + 1$  and  $m \geq 2(1 + 2^{1/\tau})$ . Let the number  $p$  of plane wave propagation directions be chosen as  $p = (m + 1)^2$ .

For ease of notation, in the rest of the paper, we set

$$\mathcal{F}(\mathbf{u}, \mathbf{f}, r + 1) = \|\nabla \cdot \mathbf{u}^{(2)}\|_{r+1,\omega,\Omega} + \|\nabla \times \mathbf{u}^{(2)}\|_{r+1,\omega,\Omega} + \sum_{l=0}^{r-1} \omega^{r-1-l} \|\mathbf{f}\|_{l,\Omega_{\tilde{s}}}.$$

### 5.2.1 The error estimates of the approximations $\mathbf{u}_h$ in the mesh-dependent norm

To derive the approximation estimates of  $\mathbf{u}^{(2)}$  in the mesh-dependent norm, we need to recall the following fundamental approximation result [see (Moiola 2013, Theorem 3.2)].

**Lemma 5.3** *Assume that the analytical solution  $\mathbf{u}^{(2)}$  of the elastic wave problems (3.4)–(3.5) belongs to  $\mathbf{H}^{r+1}(\text{div}; \Omega) \cap \mathbf{H}^{r+1}(\text{curl}; \Omega)$  ( $r \in \mathbb{N}$ ). There exists  $\xi_h \in \mathbf{V}_p^P(\mathcal{T}_h) + \mathbf{V}_p^S(\mathcal{T}_h)$  such that, for  $1 \leq j \leq r + 1$ ,*

$$\|\mathbf{u}^{(2)} - \xi_h\|_{j-1,\omega,K} \leq C\omega^{-2} \left(\frac{h}{m^\lambda}\right)^{r+1-j} \left(\|\nabla \cdot \mathbf{u}^{(2)}\|_{r+1,\omega,K} + \|\nabla \times \mathbf{u}^{(2)}\|_{r+1,\omega,K}\right), \tag{5.19}$$

where  $C$  is a constant independent of  $p$  but dependent on  $\omega$  and  $h$  only through the product  $\omega h$  as an increasing function, and may depend on the shape of the elements  $K \in \mathcal{T}_h$ ,  $r, \lambda, \mu$  and  $\rho$ .

Now, we can derive the approximation estimates of  $\mathbf{u}^{(2)}$  in the mesh-dependent norm.

**Theorem 5.2** *Assume that the analytical solution  $\mathbf{u}^{(2)}$  of the elastic wave problems (3.4)–(3.5) belongs to  $\mathbf{H}^{r+1}(\text{div}; \Omega) \cap \mathbf{H}^{r+1}(\text{curl}; \Omega)$  ( $r \in \mathbb{N}$ ). There exists  $\xi_h \in \mathbf{V}_p^P(\mathcal{T}_h) + \mathbf{V}_p^S(\mathcal{T}_h)$  such that*

$$\|\|\mathbf{u}^{(2)} - \xi_h\|\|_{\mathcal{F}_h^+} \leq C\omega^{-2} \left(\frac{h}{m^\lambda}\right)^{r-\frac{1}{2}} \left(\|\nabla \cdot \mathbf{u}^{(2)}\|_{r+1,\omega,\Omega} + \|\nabla \times \mathbf{u}^{(2)}\|_{r+1,\omega,\Omega}\right), \tag{5.20}$$

where  $C$  is a constant independent of  $p$  but dependent on  $\omega$  and  $h$  only through the product  $\omega h$  as an increasing function, and may depend on the shape of the elements  $K \in \mathcal{T}_h$ ,  $r, \lambda, \mu$  and  $\rho$ .

**Proof** Let  $\xi_h \in \mathbf{V}_p(\mathcal{T}_h)$  be defined by Lemma 5.3. For ease of notation, set  $\mathbf{e}_h = \mathbf{u}^{(2)} - \xi_h$ . By the definition of the norm  $\|\|\cdot\|\|_{\mathcal{F}_h^+}$ , we get

$$\|\|\mathbf{e}_h\|\|_{\mathcal{F}_h^+}^2 \leq C \sum_{r=1}^N \left\{ \int_{\partial\Omega_r} |\sigma(\mathbf{e}_h)|^2 + |\mathbf{e}_h|^2 \right\}. \tag{5.21}$$

Using the trace inequality, we prove by Lemma 5.3 that

$$\int_{\partial\Omega_r} |\sigma(\mathbf{e}_h)|^2 + |\mathbf{e}_h|^2 \leq C\omega^{-4} \left(\frac{h}{m^\lambda}\right)^{2r-1} \left(\|\nabla \cdot \mathbf{u}^{(2)}\|_{r+1,\omega,K}^2 + \|\nabla \times \mathbf{u}^{(2)}\|_{r+1,\omega,K}^2\right).$$

□



Based on the previous lemmas, we can derive the error estimates of the approximations  $\mathbf{u}_h^{(2)}$  and  $\mathbf{u}_h$  in the mesh-dependent norm.

**Theorem 5.3** Assume that the analytical solution  $\mathbf{u}$  of the elastic wave problems (2.1)-(2.2) belongs to  $\mathbf{H}^{r+1}(\text{div}; \Omega) \cap \mathbf{H}^{r+1}(\text{curl}; \Omega)$  ( $r \in \mathbb{N}$ ), and  $c_0 \leq h\omega \leq C_0$ . Let  $q \geq 2$ ,  $2 < r + 1 \leq \min\{\frac{m+1}{2}, q + 1\}$ , and  $\mathbf{u}_h = \mathbf{u}_h^{(1)} + \mathbf{u}_h^{(2)}$  be the approximation solution of the PWDG-LSFE. Then, for large  $p = (m + 1)^2$ , we have

$$\| \mathbf{u}^{(2)} - \mathbf{u}_h^{(2)} \|_{\mathcal{F}_h}, \| \mathbf{u} - \mathbf{u}_h \|_{\mathcal{F}_h} \leq C \left( \omega^{-2} \left( \frac{h}{m^\lambda} \right)^{r-\frac{1}{2}} + \left( \frac{h}{q} \right)^{r-\frac{1}{2}} \right) \mathcal{F}(\mathbf{u}, \mathbf{f}, r + 1), \tag{5.22}$$

where  $C$  is a constant independent of  $p$  but dependent on  $\omega$  and  $h$  only through the product  $\omega h$  as an increasing function, and may depend on the shape of the elements  $K \in \mathcal{T}_h$ ,  $r, \lambda, \mu$  and  $\rho$ .

**Proof** The PWDG formulation (3.17) is consistent by construction; thus if  $\mathbf{u}^{(2)} \in H^2(\Omega)$  solves (3.4)-(3.5), then it holds that

$$\mathcal{A}_h(\mathbf{u}^{(2)}, \mathbf{v}_h) = \ell_h(\mathbf{v}_h), \quad \forall \mathbf{v}_h \in \mathbf{V}_p(\mathcal{T}_h). \tag{5.23}$$

From (3.17) and (5.23), we have

$$\mathcal{A}_h(\mathbf{u}^{(2)} - \mathbf{u}_h^{(2)}, \mathbf{v}_h) = \mathcal{A}_h(\mathbf{u}_h^{(1)} - \mathbf{u}^{(1)}, \mathbf{v}_h), \quad \forall \mathbf{v}_h \in \mathbf{V}_p(\mathcal{T}_h). \tag{5.24}$$

Let  $\xi_h$  be the plane wave approximation defined in Theorem 5.2. It follows by (5.24) that

$$\mathcal{A}_h(\mathbf{u}^{(2)} - \mathbf{u}_h^{(2)}, \xi_h - \mathbf{u}_h^{(2)}) = \mathcal{A}_h(\mathbf{u}_h^{(1)} - \mathbf{u}^{(1)}, \xi_h - \mathbf{u}_h^{(2)}).$$

Then, by the direct manipulation, we can deduce that

$$\begin{aligned} \mathcal{A}_h(\mathbf{u}^{(2)} - \mathbf{u}_h^{(2)}, \mathbf{u}^{(2)} - \mathbf{u}_h^{(2)}) &= \mathcal{A}_h(\mathbf{u}^{(2)} - \mathbf{u}_h^{(2)}, \mathbf{u}^{(2)} - \xi_h) \\ &\quad + \mathcal{A}_h(\mathbf{u}^{(1)} - \mathbf{u}_h^{(1)}, \mathbf{u}^{(2)} - \xi_h) + \mathcal{A}_h(\mathbf{u}^{(1)} - \mathbf{u}_h^{(1)}, \mathbf{u}_h^{(2)} - \mathbf{u}^{(2)}). \end{aligned}$$

Set  $\varepsilon_h^{(1)} = \mathbf{u}^{(1)} - \mathbf{u}_h^{(1)}$  and  $\varepsilon_h^{(2)} = \mathbf{u}^{(2)} - \xi_h$ . By taking the imaginary part of the last equation and Lemma 3.1, we obtain

$$\begin{aligned} \| \mathbf{u}^{(2)} - \mathbf{u}_h^{(2)} \|_{\mathcal{F}_h}^2 &\leq | \mathcal{A}_h(\varepsilon_h^{(1)}, \varepsilon_h^{(2)}) | + | \mathcal{A}_h(\mathbf{u}^{(2)} - \mathbf{u}_h^{(2)}, \varepsilon_h^{(2)}) | + | \mathcal{A}_h(\varepsilon_h^{(1)}, \mathbf{u}_h^{(2)} - \mathbf{u}^{(2)}) | \\ &= | \mathcal{A}_h(\varepsilon_h^{(1)}, \varepsilon_h^{(2)}) | + \left| \overline{\mathcal{A}_h(\varepsilon_h^{(2)}, \mathbf{u}^{(2)} - \mathbf{u}_h^{(2)})} \right| + | \mathcal{A}_h(\varepsilon_h^{(1)}, \mathbf{u}_h^{(2)} - \mathbf{u}^{(2)}) | \\ &\leq \| \varepsilon_h^{(1)} \|_{\mathcal{F}_h^+} \| \varepsilon_h^{(2)} \|_{\mathcal{F}_h} + \| \varepsilon_h^{(2)} \|_{\mathcal{F}_h^+} \| \mathbf{u}^{(2)} - \mathbf{u}_h^{(2)} \|_{\mathcal{F}_h} + \| \varepsilon_h^{(1)} \|_{\mathcal{F}_h^+} \| \mathbf{u}^{(2)} - \mathbf{u}_h^{(2)} \|_{\mathcal{F}_h} \\ &\leq \| \varepsilon_h^{(1)} \|_{\mathcal{F}_h^+} \| \varepsilon_h^{(2)} \|_{\mathcal{F}_h^+} + (\| \varepsilon_h^{(1)} \|_{\mathcal{F}_h^+} + \| \varepsilon_h^{(2)} \|_{\mathcal{F}_h^+}) \| \mathbf{u}^{(2)} - \mathbf{u}_h^{(2)} \|_{\mathcal{F}_h}. \end{aligned} \tag{5.25}$$

It can be verified directly by (5.25) that

$$\| \mathbf{u}^{(2)} - \mathbf{u}_h^{(2)} \|_{\mathcal{F}_h} \leq \frac{\sqrt{2} + 1}{2} (\| \varepsilon_h^{(1)} \|_{\mathcal{F}_h^+} + \| \varepsilon_h^{(2)} \|_{\mathcal{F}_h^+}). \tag{5.26}$$

Notice that  $\mathbf{u}^{(2)}|_{\Omega_k} = (\mathbf{u} - \mathbf{u}^{(1)})|_{\Omega_k}$ . By the assumptions and Lemma 5.1, we have  $\mathbf{u}^{(2)}|_{\Omega_k} \in \mathbf{H}^{r+1}(\Omega_k)$  for each  $k$ . Combining (5.26) and Theorems 5.1, 5.2, gives the desired result (5.22).  $\square$

### 5.2.2 $L^2$ error estimates of the approximations $\mathbf{u}_h$

To prove an error estimate in  $L^2(\Omega)$  for the PWDG method, we adopt the approach from Buffa and Monk (2008), Cummings and Feng (2006), Hiptmair et al. (2011), Luostari et al. (2013). Considering the dual (nonhomogeneous) problem of the Navier equation (2.1) (see Cummings and Feng 2006)

$$\begin{cases} \mu \Delta \mathbf{v} + (\lambda + \mu) \nabla(\nabla \cdot \mathbf{v}) + \omega^2 \rho \mathbf{v} = \boldsymbol{\psi} & \text{in } \Omega \\ \mathbf{T}^{(\mathbf{n})}(\mathbf{v}) - i\eta \mathbf{v} = \mathbf{0} & \text{on } \gamma = \partial\Omega, \end{cases} \tag{5.27}$$

where  $\boldsymbol{\psi} \in \mathbf{L}^2(\Omega)$ . Let us recall the regularity estimates for the elastic wave problem proved in Cummings and Feng (2006).

**Lemma 5.4** (Cummings and Feng 2006, Theorem 2) *Let  $\Omega$  be a convex polyhedron or smooth domain. Then the following regularity estimates for  $\mathbf{v}$  hold:*

$$\begin{cases} \|\mathbf{v}\|_{1,\Omega} \leq C(1 + \omega + \frac{1}{\omega^2})\|\boldsymbol{\psi}\|_{0,\Omega}, \\ \|\mathbf{v}\|_{2,\Omega} \leq C(1 + \omega^2 + \frac{1}{\omega^2})\|\boldsymbol{\psi}\|_{0,\Omega}. \end{cases} \tag{5.28}$$

We can prove the following error estimate using duality. We underline that the proof is based on the technique from (Luostari et al. 2013, Theorem 3.13). For completeness, we give the detailed proof.

**Lemma 5.5** *Assuming  $\Omega$  be a convex polyhedron and covered by a regular and quasi-uniform mesh, then there exists a constant  $C > 0$  independent of  $\omega, h$ , and  $\mathbf{w}$  such that for any  $\mathbf{w} \in \mathbf{V}(\mathcal{T}_h)$ ,*

$$\|\mathbf{w}\|_{0,\Omega} \leq C\omega^{\frac{3}{2}}\|\mathbf{w}\|_{\mathcal{F}_h}. \tag{5.29}$$

**Proof** Let  $\mathbf{v}$  satisfy the dual problem (5.27). Integrating by parts, using the definition of the Trefftz space  $\mathbf{V}(\mathcal{T}_h)$  and the relation  $\boldsymbol{\sigma}(\mathbf{v}) : \nabla \mathbf{w} = \nabla \mathbf{v} : \boldsymbol{\sigma}(\mathbf{w})$ , we obtain

$$\begin{aligned} (\mathbf{w}, \boldsymbol{\psi}) &= \sum_{k=1}^N \int_{\Omega_k} (-\nabla \mathbf{w} : \boldsymbol{\sigma}(\bar{\mathbf{v}}) + \mathbf{w} \cdot \omega^2 \rho \bar{\mathbf{v}}) \, d\mathbf{x} + \sum_{k=1}^N \int_{\partial\Omega_k} \mathbf{w} \cdot \boldsymbol{\sigma}(\bar{\mathbf{v}}) \, \mathbf{n} \, dS \\ &= \sum_{k=1}^N \int_{\Omega_k} (-\boldsymbol{\sigma}(\mathbf{w}) : \nabla \bar{\mathbf{v}} + \mathbf{w} \cdot \omega^2 \rho \bar{\mathbf{v}}) \, d\mathbf{x} + \sum_{k=1}^N \int_{\partial\Omega_k} \mathbf{w} \cdot \boldsymbol{\sigma}(\bar{\mathbf{v}}) \, \mathbf{n} \, dS \\ &= \sum_{k=1}^N \int_{\Omega_k} ((\nabla \cdot \boldsymbol{\sigma}(\mathbf{w}) + \omega^2 \rho \mathbf{w}) \cdot \bar{\mathbf{v}}) \, d\mathbf{x} + \sum_{k=1}^N \int_{\partial\Omega_k} (\mathbf{w} \cdot \boldsymbol{\sigma}(\bar{\mathbf{v}}) \mathbf{n} - \boldsymbol{\sigma}(\bar{\mathbf{w}}) \mathbf{n} \cdot \bar{\mathbf{v}}) \, dS \\ &= \sum_{k=1}^N \int_{\partial\Omega_k} (\mathbf{w} \cdot \boldsymbol{\sigma}(\bar{\mathbf{v}}) \mathbf{n} - \boldsymbol{\sigma}(\mathbf{w}) \mathbf{n} \cdot \bar{\mathbf{v}}) \, dS. \end{aligned}$$

Recalling the definition of the jumps  $[[\mathbf{w}]]$  and  $[[\boldsymbol{\sigma}(\mathbf{w})]]$  in (3.8) and taking into account the boundary condition of (5.27), we obtain

$$\begin{aligned} (\mathbf{w}, \boldsymbol{\psi}) &= \sum_{\Gamma_{ij}, i < j} \int_{\Gamma_{ij}} ([[ \mathbf{w} ]] \mathbf{n} \cdot \overline{\boldsymbol{\sigma}(\mathbf{v}) \mathbf{n}} - [[ \boldsymbol{\sigma}(\mathbf{w}) ]] \cdot \bar{\mathbf{v}}) \, dS \\ &\quad + \sum_{\gamma_k \in \gamma} \int_{\gamma_k} (\mathbf{w} \cdot \overline{\boldsymbol{\sigma}(\mathbf{v}) \mathbf{n}} - \boldsymbol{\sigma}(\mathbf{w}) \mathbf{n} \cdot \bar{\mathbf{v}}) \, dS \end{aligned}$$

$$\begin{aligned}
 &= \sum_{\Gamma_{ij}, l < j} \int_{\Gamma_{ij}} \left( [[\mathbf{w}]] \mathbf{n} \cdot \overline{\boldsymbol{\sigma}(\mathbf{v}) \mathbf{n}} - [[\boldsymbol{\sigma}(\mathbf{w})]] \cdot \overline{\mathbf{v}} \right) dS \\
 &\quad + \sum_{\gamma_k \in \mathcal{Y}} \int_{\gamma_k} \left( \mathbf{w} \cdot i \eta \overline{\mathbf{v}} - \boldsymbol{\sigma}(\mathbf{w}) \mathbf{n} \cdot \overline{\mathbf{v}} \right) dS \\
 &= \sum_{\Gamma_{ij}, l < j} \int_{\Gamma_{ij}} \left( \alpha^{\frac{1}{2}} [[\mathbf{w}]] \mathbf{n} \cdot \overline{\alpha^{-\frac{1}{2}} \boldsymbol{\sigma}(\mathbf{v}) \mathbf{n}} - \beta^{\frac{1}{2}} [[\boldsymbol{\sigma}(\mathbf{w})]] \cdot \overline{\beta^{-\frac{1}{2}} \mathbf{v}} \right) dS \\
 &\quad - \sum_{\gamma_k \in \mathcal{Y}} \int_{\Gamma_{ij}} \left( i(1 - \delta)^{\frac{1}{2}} \eta^{\frac{1}{2}} \mathbf{w} \cdot \overline{(1 - \delta)^{-\frac{1}{2}} \eta^{\frac{1}{2}} \mathbf{v}} + \delta^{\frac{1}{2}} \eta^{-\frac{1}{2}} \boldsymbol{\sigma}(\mathbf{w}) \mathbf{n} \cdot \overline{\delta^{-\frac{1}{2}} \eta^{\frac{1}{2}} \mathbf{v}} \right) dS,
 \end{aligned}$$

where  $\mathbf{n}$  denotes the unit normal vector pointing from  $\Omega_l$  to  $\Omega_j$ . By Cauchy–Schwarz inequality, we have

$$\begin{aligned}
 |(\mathbf{w}, \boldsymbol{\psi})| &\leq \sum_{\Gamma_{ij}, l < j} \left( \|\alpha^{\frac{1}{2}} [[\mathbf{w}]] \mathbf{n}\|_{0, \Gamma_{ij}} \|\alpha^{-\frac{1}{2}} \boldsymbol{\sigma}(\mathbf{v}) \mathbf{n}\|_{0, \Gamma_{ij}} + \|\beta^{\frac{1}{2}} [[\boldsymbol{\sigma}(\mathbf{w})]]\|_{0, \Gamma_{ij}} \|\beta^{-\frac{1}{2}} \mathbf{v}\|_{0, \Gamma_{ij}} \right) \\
 &\quad + \sum_{\gamma_k \in \mathcal{Y}} \left( \|(1 - \delta)^{\frac{1}{2}} \eta^{\frac{1}{2}} \mathbf{w}\|_{0, \gamma_k} \|(1 - \delta)^{-\frac{1}{2}} \eta^{\frac{1}{2}} \mathbf{v}\|_{0, \gamma_k} \right. \\
 &\quad \left. + \|\delta^{\frac{1}{2}} \eta^{-\frac{1}{2}} \boldsymbol{\sigma}(\mathbf{w}) \mathbf{n}\|_{0, \gamma_k} \|\delta^{-\frac{1}{2}} \eta^{\frac{1}{2}} \mathbf{v}\|_{0, \gamma_k} \right) \leq \| \mathbf{w} \|_{\mathcal{F}_h} \cdot G^{\frac{1}{2}}, \tag{5.30}
 \end{aligned}$$

where  $G$  is defined by

$$\begin{aligned}
 G &= \sum_{\Gamma_{ij}, l < j} \left( \|\alpha^{-\frac{1}{2}} \boldsymbol{\sigma}(\mathbf{v}) \mathbf{n}\|_{0, \Gamma_{ij}}^2 + \|\beta^{-\frac{1}{2}} \mathbf{v}\|_{0, \Gamma_{ij}}^2 \right) \\
 &\quad + \sum_{\gamma_k \in \mathcal{Y}} \left( \|(1 - \delta)^{-\frac{1}{2}} \eta^{\frac{1}{2}} \mathbf{v}\|_{0, \gamma_k}^2 + \|\delta^{-\frac{1}{2}} \eta^{\frac{1}{2}} \mathbf{v}\|_{0, \gamma_k}^2 \right). \tag{5.31}
 \end{aligned}$$

By  $\|\eta\|_{\infty} \leq C\omega$  and  $\|\eta^{-1}\|_{\infty} \leq C\omega^{-1}$ , and applying the trace inequality and the regularity estimates (5.28), we further get the following estimate

$$\begin{aligned}
 G &\leq C \sum_k \left( \omega \|\nabla \mathbf{v}\|_{0, \Omega_k}^2 + \omega \|\mathbf{v}\|_{0, \Omega_k}^2 + h \|\nabla \boldsymbol{\sigma}(\mathbf{v})\|_{0, \Omega_k}^2 + h^{-1} \|\boldsymbol{\sigma}(\mathbf{v})\|_{0, \Omega_k}^2 \right) \\
 &\leq C\omega \|\mathbf{v}\|_{1, \Omega}^2 + h \|\mathbf{v}\|_{2, \Omega}^2 \leq C\omega^3 \|\boldsymbol{\psi}\|_{0, \Omega}^2. \tag{5.32}
 \end{aligned}$$

Taking (5.32) into (5.30) and choosing  $\boldsymbol{\psi} = \mathbf{w}$ , we obtain the estimate (5.29).

Combining Lemma 5.5 with Theorem 5.3, we obtain an error estimate in  $L^2(\Omega)$  for our method. □

**Theorem 5.4** *Under the assumption of Theorem 5.3 and Lemma 5.5, Let  $q \geq 2, 2 < r + 1 \leq \min\{\frac{m+1}{2}, q + 1\}$ , and  $\mathbf{u}_h = \mathbf{u}_h^{(1)} + \mathbf{u}_h^{(2)}$  be the approximation solution of the PWDG–LSFE. Then, for large  $p = (m + 1)^2$ , we have*

$$\|\mathbf{u} - \mathbf{u}_h\|_{0, \Omega} \leq C \left( \omega^{-\frac{1}{2}} \left( \frac{h}{m^\lambda} \right)^{r-\frac{1}{2}} + \omega^{\frac{3}{2}} \left( \frac{h}{q} \right)^{r-\frac{1}{2}} \right) \mathcal{F}(\mathbf{u}, \mathbf{f}, r + 1), \tag{5.33}$$

where  $C$  is a constant independent of  $p, \mathbf{u}$  but dependent on  $\omega$  and  $h$  only through the product  $\omega h$  as an increasing function, and may depend on the shape of the elements  $K \in \mathcal{T}_h, r, \lambda, \mu$  and  $\rho$ .

### 5.3 Error estimate of the plane wave approximations for two-dimensional case

Let the mesh triangulation  $\mathcal{T}_h$  satisfy the shape regularity and quasi-uniformity, and set  $p = 2m + 1$ , where the  $p$  directions  $\{\mathbf{d}_l = (\cos\theta_l, \sin\theta_l)\}_{l=1}^p$  satisfy the following condition: there exists  $\zeta \in (0, 1]$  such that the minimum angle between two different directions is greater than or equal to  $2\pi\zeta/p$ .

By the plane wave approximation theory in Hiptmair et al. (2011) and (Moiola 2013, Theorem 3.2), we can obtain the following approximation.

**Lemma 5.6** *Assume that the analytical solution  $\mathbf{u}^{(2)}$  of the elastic wave problems (3.4)–(3.5) belongs to  $\mathbf{H}^{r+1}(\text{div}; \Omega) \cap \mathbf{H}^{r+1}(\text{curl}; \Omega)$  ( $r \in \mathbb{N}$ ). There exists  $\xi_h \in \mathbf{V}_p^P(\mathcal{T}_h) + \mathbf{V}_p^S(\mathcal{T}_h)$  such that, for  $1 \leq j \leq r + 1$ ,*

$$\begin{aligned} \|\mathbf{u}^{(2)} - \xi_h\|_{j-1, \omega, K} &\leq C\omega^{-2}h^{r+1-j} \left(\frac{\log(p)}{p}\right)^{r+1-j} \\ &\left(\|\nabla \cdot \mathbf{u}^{(2)}\|_{r+1, \omega, K} + \|\nabla \times \mathbf{u}^{(2)}\|_{r+1, \omega, K}\right), \end{aligned} \tag{5.34}$$

where  $C$  is a constant independent of  $p$  but dependent on  $\omega$  and  $h$  only through the product  $\omega h$  as an increasing function, and may depend on the shape of the elements  $K \in \mathcal{T}_h$ ,  $r$ ,  $\lambda$ ,  $\mu$  and  $\rho$ .

Now we get the error estimates for our method, as in the proof of Theorems 5.3 and 5.4.

**Theorem 5.5** *Let  $q \geq 2$ ,  $2 < r + 1 \leq \min\{\frac{m+1}{2}, q + 1\}$ . Assume that  $c_0 \leq h\omega \leq C_0$ ,  $\mathbf{f} \in \mathbf{H}^{r-1}(\Omega)$  and  $\mathbf{u} \in \mathbf{H}^{r+1}(\text{div}; \Omega) \cap \mathbf{H}^{r+1}(\text{curl}; \Omega)$  ( $r \in \mathbb{N}$ ). Then*

$$\begin{aligned} &\|\|\mathbf{u}^{(2)} - \mathbf{u}_h^{(2)}\|\|_{\mathcal{F}_h}, \|\|\mathbf{u} - \mathbf{u}_h\|\|_{\mathcal{F}_h} \\ &\leq C \left(\omega^{-2}h^{r-\frac{1}{2}} \left(\frac{\log(p)}{p}\right)^{r-\frac{1}{2}} + \left(\frac{h}{q}\right)^{r-\frac{1}{2}}\right) \mathcal{F}(\mathbf{u}, \mathbf{f}, r + 1), \end{aligned} \tag{5.35}$$

and

$$\|\|\mathbf{u} - \mathbf{u}_h\|\|_{0, \Omega} \leq C \left(\omega^{-\frac{1}{2}}h^{r-\frac{1}{2}} \left(\frac{\log(p)}{p}\right)^{r-\frac{1}{2}} + \omega^{\frac{3}{2}}\left(\frac{h}{q}\right)^{r-\frac{1}{2}}\right) \mathcal{F}(\mathbf{u}, \mathbf{f}, r + 1). \tag{5.36}$$

**Remark 5.2** We mention that all theoretical results are dependent on the assumption  $\omega h \geq c_0$ . Thus, they do not provide orders of asymptotic convergence with respect to  $h$  when the meshwidth  $h$  becomes much smaller. The  $h$ -convergence orders described herein are under the restriction of such assumption  $h \geq c_0/\omega$ .

**Remark 5.3** The error estimates given in Theorems 5.3, 5.4 and 5.5 are obtained only for the case of the number of  $S$ -wave basis functions  $p_0$  equaling the number of  $P$ -wave basis functions  $p_1$ . Indeed, as already mentioned in Huttunen et al. (2004), to obtain the best accuracy, the ratio of the number of  $S$ - and  $P$ -wave basis functions  $p_0/p_1$  should be about the ratio of  $S$ - and  $P$ -wavenumbers  $\kappa_S/\kappa_P$ . Furthermore, we can derive the corresponding error estimates by proceeding as in Theorems 5.3, 5.4 and 5.5.

**Remark 5.4** The error estimates given in Theorems 5.3, 5.4 and 5.5 are also established for the homogeneous elastic wave equations, where error estimates of the local spectral element approximations are eliminated.

## 6 Numerical experiments

We simply choose constant parameters ( $\alpha = \beta = \delta = 1/2$ ) to solve time-harmonic elastic wave problems (2.1), (2.2) in two-dimensional and three-dimensional homogeneous media, and we report some numerical results to verify the validity of the theoretical results.

A uniform triangulation  $\mathcal{T}_h$  is employed for the domain  $\Omega$  for the examples as follows:  $\Omega$  is divided into small rectangles or cubes of equal meshwidth, where  $h$  is the length of the longest edge of the elements. We choose the number  $p$  of basis functions on all elements  $\{\Omega_k\}$  to be  $p = 2m + 1$  for two-dimensional case and  $p = (m + 1)^2$  for three-dimensional case, where  $m$  is a variable positive integer.

To measure the accuracy of the numerical solution  $\mathbf{u}_h$ , we introduce the following relative numerical error:

$$\text{err.} = \frac{\|\mathbf{u} - \mathbf{u}_h\|_{L^2(\Omega)}}{\|\mathbf{u}\|_{L^2(\Omega)}} \tag{6.1}$$

for the exact solution  $\mathbf{u} \in (L^2(\Omega))^d$ .

### 6.1 Rayleigh waves

Since discretization of the PWDG method in this study uses  $P$ - and  $S$ -plane waves only, it is vital to investigate whether the method can resolve surface waves that are not explicitly contained in the basis for the PWDG. To do this we study Rayleigh waves in the square domain  $\Omega = [0, 1]^2$ . The exact expression for the Rayleigh wave speed  $C_R$  is somewhat complicated; therefore, we use the approximation value from Auld (1973) given by

$$C_R = \frac{0.87 + 1.12\nu}{1 + \nu} C_S.$$

We denote the Rayleigh wavenumber by  $\kappa_R = \omega/C_R$ .

The  $x$  and  $y$  components of the displacement field  $\mathbf{u} = (u_x, u_y)^T$  can be written as follows (see Auld 1973 for details):

$$\begin{cases} u_x = \alpha_S \{ e^{-\alpha_S y} - \frac{2\kappa_R^2}{\kappa_R^2 + \alpha_S^2} e^{-\alpha_P y} \} e^{i\kappa_R x} \\ u_y = i\kappa_R \{ e^{-\alpha_S y} - \frac{2\alpha_P \alpha_S}{\kappa_R^2 + \alpha_S^2} e^{-\alpha_P y} \} e^{i\kappa_R x}, \end{cases} \tag{6.2}$$

where

$$\alpha_P = \sqrt{\kappa_R^2 - \kappa_P^2} \quad \text{and} \quad \alpha_S = \sqrt{\kappa_R^2 - \kappa_S^2}$$

Elastic properties of the medium occupying the domain  $\Omega$  are taken to be those of steel ( $E = 200 \times 10^9$ ,  $\nu = 0.3$ , and  $\rho = 7800$ ). Hence,  $S$ - and  $P$ - wave speeds are  $C_P = 5875$  and  $C_S = 3140$ , respectively. This gives a ratio  $C_P/C_S = \kappa_S/\kappa_P = 1.87$ . Single-frequency examples for this first model problem are computed with  $f = 2z \times 10^4$  ( $z \in \mathbb{N}$ ), which corresponds to  $\omega = 4\pi z \times 10^4$  and  $\kappa_P = 21.4z$ . These parameters are not motivated by any particular application, but the ratio  $C_P/C_S$  is typical for a wide range of solid materials.

Table 1 and Fig. 1 show the errors of the numerical solutions in  $\mathcal{F}_h$ -norm and relative  $L^2$ -norm with respect to  $p$ , where the direct method is employed to solve the discrete system. A fairly coarse mesh  $h = \frac{1}{4}$  when  $\kappa_P = 21.4$  is used. We choose the number  $p$  of basis functions from  $p = 17$  to  $p = 27$ .

**Table 1** Errors of the approximations with respect to  $p$

$p$	17	19	21	23	25	27
$\ u - u_h\ _{\mathcal{F}_h}$	$7.98e-3$	$6.93e-3$	$4.31e-3$	$2.21e-3$	$1.20e-3$	$5.86e-4$
Err.	$3.38e-1$	$2.21e-1$	$1.19e-1$	$5.30e-2$	$2.46e-2$	$1.27e-2$

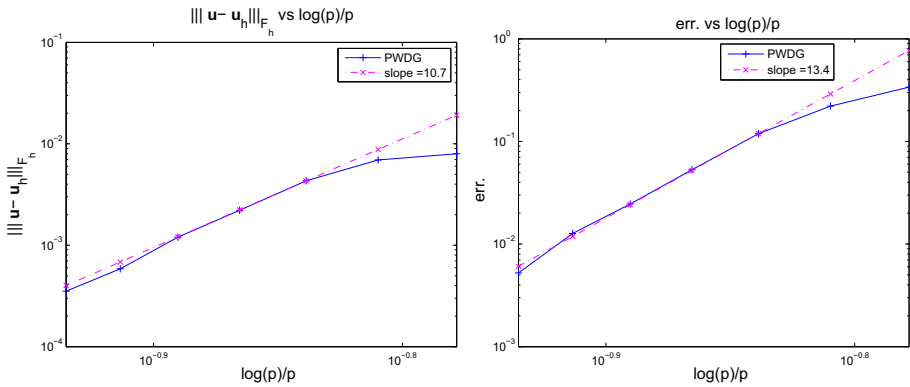


**Fig. 1** Left:  $\|u - u_h\|_{\mathcal{F}_h}$  vs  $\log(p)/p$ . Right:  $\text{err.}$  vs  $\log(p)/p$

**Table 2** Errors of the approximations with respect to  $h$  when  $\kappa p = 21.4$  and  $p = 15$

$h$	$\frac{1}{4}$	$\frac{1}{6}$	$\frac{1}{8}$	$\frac{1}{10}$	$\frac{1}{12}$	$\frac{1}{14}$
$\ u - u_h\ _{\mathcal{F}_h}$	$8.80e-3$	$4.70e-3$	$1.50e-3$	$4.89e-4$	$1.90e-4$	$8.13e-5$
err.	$4.79e-1$	$1.14e-1$	$2.17e-2$	$5.40e-3$	$1.70e-3$	$6.08e-4$

Figure 1 shows the plot of  $\|u - u_h\|_{\mathcal{F}_h}$  and  $\text{err.}$  with respect to  $\frac{\log(p)}{p}$ , respectively. It highlights two different regimes for increasing  $p$ : (i) a preasymptotic region with slow convergence, (ii) a region of faster convergence with a linear plot which verifies the validity of the theoretical results in Theorem 5.5. As stated in Remark 3.14 (see Hiptmair et al. 2011), the convergence order of the approximations with respect to  $p$  turns out to be exponential since the analytical solution of the problem can be extended analytically outside the domain.

Table 2 and Fig. 2 show the errors of the numerical solutions in  $\mathcal{F}_h$ -norm and relative  $L^2$ -norm with respect to  $h$ .

We can see from Fig. 2 that it displays a linear plot which verifies the validity of the theoretical results in Theorem 5.5. Particularly, due to the best approximation error adopted in the proof of the theoretical estimates, the convergence order of the approximations with respect to  $h$  is not exponential but algebraic.

### 6.2 Wave propagation

For the second example, we study elastic wave propagation through a cube  $\Omega = [0, 1]^3$ . The exact solution of the problems is a plane wave consisting both  $P$ - and  $S$ - waves:

$$u^{\text{inc}} = a \exp(i\kappa p a \cdot x) + b \exp(i\kappa_S a \cdot x) + c \exp(i\kappa_S a \cdot x). \tag{6.3}$$

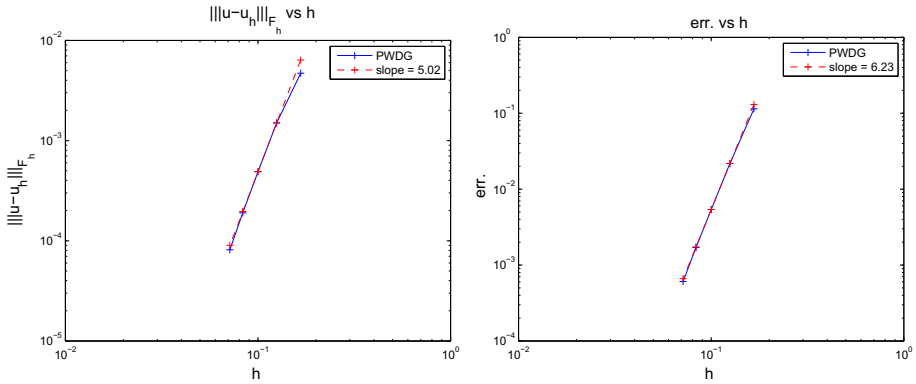


**Fig. 2** Left :  $h$ -convergence in  $\mathcal{F}_h$ -norm in logarithmic scale. Right:  $h$ -convergence in relative  $L^2$ -norm in logarithmic scale

**Table 3** Errors of the approximations with respect to  $p$

$p$	16	25	36	49	64
$    \mathbf{u} - \mathbf{u}_h    _{\mathcal{F}_h}$	1.02e+1	1.93	3.40e-1	6.46e-2	1.04e-2
err.	2.99e-2	3.67e-3	4.77e-4	7.39e-5	1.17e-05
$\theta$	3.93e-1	2.13e-1	2.05e-1	2.70e-1	2.17e-1

The directions  $\mathbf{a}$ ,  $\mathbf{b}$  and  $\mathbf{c}$  are chosen so that  $\mathbf{a} \cdot \mathbf{b} = 0$  and  $\mathbf{c} = \mathbf{b} \times \mathbf{a}$ . This example is chosen because it provides a very simple problem to verify the validity of the theoretical results in Theorems 5.3, 5.4 and test the accuracy of the elastic PWDG for wave propagation.

The material properties of the medium and the frequency of the wave field  $f = 0.5\zeta \times 10^4$  ( $\zeta \in \mathbb{N}$ ) are the same as those in the first test problem. The direction of the wave in all cases is  $\mathbf{a} = (\frac{1.0}{\sqrt{3}}, \frac{1.0}{\sqrt{3}}, \frac{1.0}{\sqrt{3}})^T$ . This choice does not coincide with any of the directions of the plane wave basis functions  $\mathbf{d}_l$ . We define the distance  $\theta$  between the exact solution direction  $\mathbf{a}$  and the closest plane wave propagation direction by

$$\theta = \min_{1 \leq l \leq p} ||\mathbf{a} - \mathbf{d}_l||_2.$$

The coupling parameter  $\sigma$  is given by (2.5).

Table 3 and Fig. 3 show the errors of numerical solution  $\mathbf{u}_h$  in the  $\mathcal{F}_h$ -norm and the relative  $L^2$ -norm with respect to  $m$ . A fairly coarse mesh  $h = \frac{1}{4}$  when  $\kappa_P = 5.35$  is used.

Similar to the first test, Fig. 3 also highlights that the convergence order of the approximations generated by the PWDG method with respect to  $m$  turns out to be exponential.

Table 4 shows the errors of numerical solution  $\mathbf{u}_h$  in the  $\mathcal{F}_h$ -norm and the relative  $L^2$ -norm. The results listed in Table 4 indicate that the approximations generated by the plane wave methods possess high accuracy when the mesh size  $h$  decreases.

Figure 4 shows the plots of  $h$ -convergence orders of the  $\mathcal{F}_h$ -norm errors and the relative  $L^2$ -norm errors, respectively. The plots highlight regions of high-order convergence for decreasing  $h$  for the PWDG method.

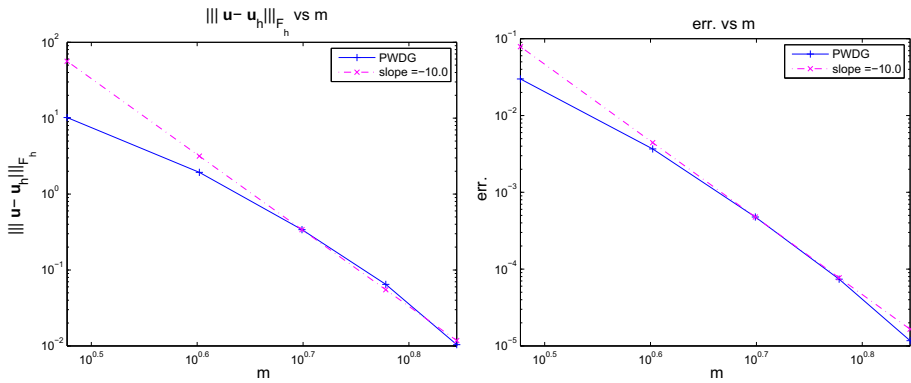


Fig. 3 Left:  $|||u - u_h|||_{\mathcal{F}_h}$  vs  $m$ . Right:  $err.$  vs  $m$

Table 4 Errors of the approximations with respect to  $h$  when  $\kappa p = 5.35$  and  $p = 16$

$h$	$\frac{1}{3}$	$\frac{1}{4}$	$\frac{1}{5}$	$\frac{1}{6}$	$\frac{1}{7}$	$\frac{1}{8}$
$   u - u_h   _{\mathcal{F}_h}$	1.78e+1	1.02e+1	6.36	4.28	3.04	2.25
err.	8.49e-2	2.99e-2	1.36e-2	7.18e-3	4.21e-3	2.64e-3

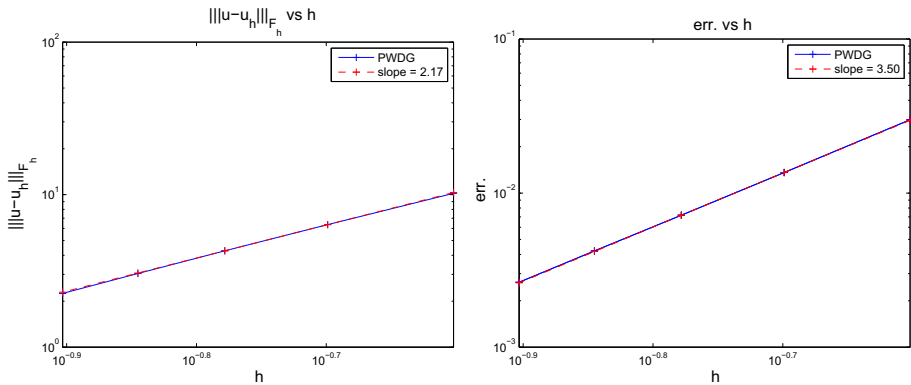


Fig. 4 Left:  $h$ -convergence in  $\mathcal{F}_h$ -norm in logarithmic scale. Right:  $h$ -convergence in relative  $L^2$ -norm in logarithmic scale

### 6.3 The two-dimensional nonhomogeneous problem

To illustrate the effectiveness of the proposed approach for general nonhomogeneous problems, we consider the nonhomogeneous elastic equations whose analytical solution is given by

$$\mathbf{u}_{ex} = (x \cos y, -y \sin x)^t. \tag{6.4}$$

In this example, the source term  $\mathbf{f}$  does not vanish over the entire computational domain  $[0, 1]^2$ . The material properties of the medium are chosen as follow.  $E = 200 \times 10$ ,  $\nu = 0.3$ ,  $\rho = 78$ ,  $f = 2z$  and  $\omega = 4\pi z$  ( $z \in \mathbb{N}$ ).



**Table 5** Errors of the approximations with respect to  $h$  when  $\omega = 16\pi$  and  $q = 3, p = 9$

$h$	$\frac{1}{4}$	$\frac{1}{6}$	$\frac{1}{8}$	$\frac{1}{10}$	$\frac{1}{12}$
$\ u - u_h\ _{\mathcal{F}_h}$	3.25	6.83e-1	1.40e-1	4.80e-2	2.41e-2
err.	4.60e-2	5.50e-3	1.20e-3	2.44e-4	1.03e-4

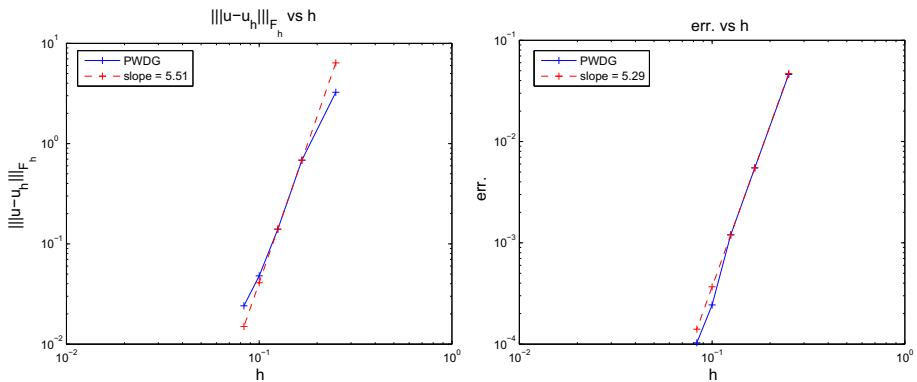


**Fig. 5** Left :  $h$ -convergence in relative  $\mathcal{F}_h$ -norm in logarithmic scale. Right:  $h$ -convergence in relative  $L^2$ -norm in logarithmic scale

**Table 6** Errors of approximations with respect to  $p$  ( $\omega = 16\pi, h = 1/8$ )

$m$	2	3	4	5
$q = 2$	1.93e-2	2.23e-2	2.38e-2	2.39e-2
$q = 3$	1.40e-2	2.70e-3	7.35e-4	7.75e-4

Table 5 and Fig. 5 show the errors of numerical solution  $u_h$  in the  $\mathcal{F}_h$ -norm and the relative  $L^2$ -norm when  $h$  decreases.

Figure 5 highlights regions of high-order convergence for decreasing  $h$  for the PWDG-LSFE.

We can also fix the mesh size  $h$ , but increase both  $p$  and  $q$ . The resulting relative  $L^2$  errors of the approximations generated by the PWDG-LSFE method are listed in Table 6.

It can be seen from the above Table that the errors in  $L^2$  relative norm decrease when  $q$  increases for the cases of  $m = 2, 3, 4, 5$ , which verifies the validity of the theoretical results given in Theorem 5.5. Moreover, the optimal value of  $m$  is  $m = 2$  (rep. 4) when  $q = 2$  (rep.  $q = 3$ ).

Besides, the errors in  $L^2$  relative norm almost stagnate for increasing  $p$ . This behavior is not a surprise: as stated in Hu and Yuan (2018), the  $L^2$  errors of  $u_h$  should be mainly determined by  $\|u^{(1)} - u_h^{(1)}\|_{0,\Omega}$  and may decrease slowly when  $p$  increases but  $q$  is fixed (unless  $q$  also increases), since  $\|u^{(1)} - u_h^{(1)}\|_{0,\Omega}$  depends on  $q$ , instead of  $p$ .

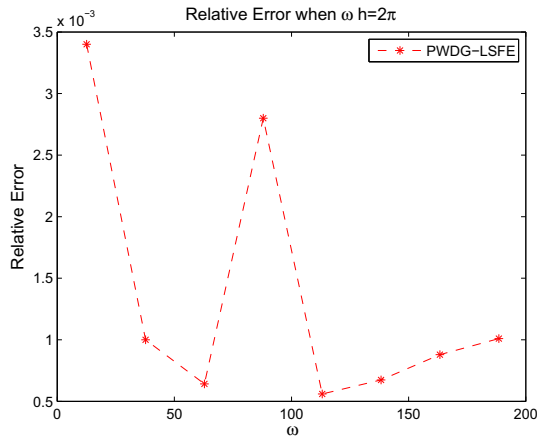
Table 7 and Fig. 6 show the the relative  $L^2$ -norm errors of the approximations with large wave numbers generated by the PWDG-LSFE.

Table 7 and Fig. 6 indicate that the approximations generated by the PWDG-LSFE have high accuracy when  $\omega$  increases for the case of the fixed value  $\omega h = 2\pi$ .

**Table 7** Errors of approximations for the case of  $\omega h = 2\pi$ ,  $p = 9$ ,  $q = 3$

$\omega$	$4\pi$	$12\pi$	$20\pi$	$28\pi$	$36\pi$	$44\pi$	$52\pi$
err.	$3.40e-3$	$1.00e-3$	$6.42e-4$	$2.80e-3$	$5.60e-4$	$6.74e-4$	$8.79e-4$

**Fig. 6** Err. vs  $\omega$



**Table 8** Errors of the approximations with respect to  $h$  when  $\omega = 10\pi$ ,  $q = 3$  and  $p = 16$

$h$	$\frac{1}{3}$	$\frac{1}{4}$	$\frac{1}{5}$	$\frac{1}{6}$	$\frac{1}{7}$	$\frac{1}{8}$
err.	$1.28e-1$	$2.28e-2$	$6.18e-3$	$2.11e-3$	$8.49e-4$	$3.86e-4$

### 6.4 The three-dimensional nonhomogeneous problem

In this section, we consider the nonhomogeneous elastic equations whose analytical solution is given by

$$\mathbf{u}_{\text{ex}} = (xz \cos y, -z \sin y, xy)^t. \tag{6.5}$$

The frequency of the wave field  $f$  and  $\omega$  are chosen as follows.  $f = z$  and  $\omega = 2\pi z$  ( $z \in \mathbb{N}$ ). The other material properties of the medium are the same as those in the third test problem.

Table 8 and Fig. 7 show the relative  $L^2$ -norm errors of the approximations when  $h$  decreases.

Figure 7 highlights regions of high-order convergence for decreasing  $h$  for the PWDG-LSFE.

We can also fix the mesh size  $h$ , but increase both  $p$  and  $q$ . The resulting relative  $L^2$  errors of the approximations generated by the PWDG- method are listed in Table 9.

It can be seen from the above Table that the errors in  $L^2$  relative norm decrease when  $q$  increases for the cases of  $m = 2, 3, 4, 5$ , which verifies the validity of the theoretical results given in Theorem 5.4. Moreover, the optimal value of  $m$  is  $m = 3$  (rep. 4) when  $q = 2$  (rep.  $q = 3$ ).

Table 10 shows the the relative  $L^2$ -norm errors of the approximations with large wave numbers generated by the PWDG-LSFE.

Table 10 and Fig. 8 indicate that the approximations generated by the PWDG-LSFE have high accuracy when  $\omega$  increases for the case of the fixed value  $\omega h = \pi$ .

**Fig. 7**  $h$ -convergence in relative  $L^2$ -norm in logarithmic scale

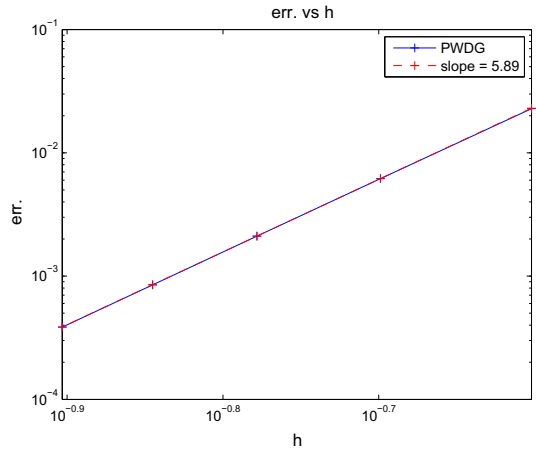


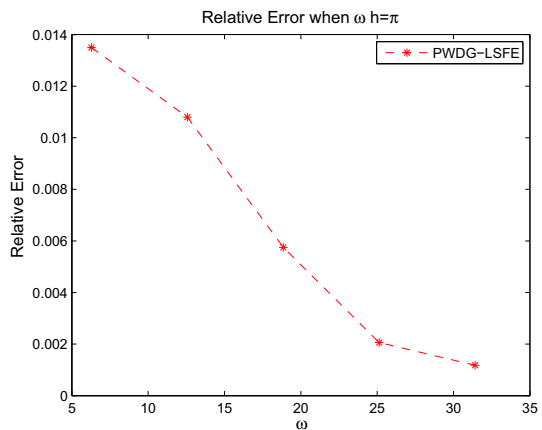
**Table 9** Errors of approximations with respect to  $p$  ( $\omega = 10\pi, h = 1/4$ )

$m$	2	3	4	5
$q = 2$	6.09e-2	6.34e-2	7.08e-2	7.23e-2
$q = 3$	7.90e-2	2.28e-2	1.52e-2	1.57e-2

**Table 10** Errors of approximations for the case of  $\omega h = \pi, p = 16, q = 2$

$\omega$	$2\pi$	$4\pi$	$6\pi$	$8\pi$	$10\pi$
err.	1.35e-2	1.08e-2	8.27e-3	2.06e-3	1.18e-3

**Fig. 8** Err. vs  $\omega$



### 7 Conclusion

In this paper, combined with local spectral element method, we have extended the PWDG method to discretize the time-harmonic elastic wave propagation problems, and derived error estimates of the numerical solutions in two and three dimensions. Numerical results verify the validity of the theoretical results, and show that the approximate solutions possess high accuracy.

**Acknowledgements** The authors wish to thank the anonymous referee for many insightful comments which led to great improvement in the results and the presentation of the paper.

## References

- Auld B (1973) Acoustic waves and fields in solids, vol 2. Wiley, New York
- Buffa A, Monk P (2008) Error estimates for the ultra weak variational formulation of the Helmholtz equation. *ESIAM* 42:925–940
- Cessenat O (1996) Application d'une nouvelle formulation variationnelle aux équations d'ondes harmoniques, Problèmes de Helmholtz 2D et de Maxwell 3D, Ph.D. Thesis, Université Paris IX Dauphine
- Cessenat O, Despres B (1998) Application of an ultra weak variational formulation of elliptic pdes to the two-dimensional helmholtz problem. *SIAM J Numer Anal* 35(1):255–299
- Cessenat O, Despres B (2003) Using plane waves as basis functions for solving time harmonic equations with the ultra weak variational formulation. *J Comput Acous* 11(2):227–238
- Cummings P, Feng X (2006) Sharp regularity coefficient estimates for complex-valued acoustic and elastic Helmholtz equations. *Math Mod Methods Appl Sci* 16:139–160
- Du Y, Wu H (2015) Preasymptotic error analysis of higher order FEM and CIP-FEM for Helmholtz equation with high wave number. *SIAM J Numer Anal* 53(2):782–804
- El Kacimi A, Laghrouche O (2009) Numerical modeling of elastic wave scattering in frequency domain by the partition of unity finite element method. *Int J Numer Methods Eng* 77:1646–1669
- El Kacimi A, Laghrouche O (2010) Improvement of PUFEM for the numerical solution of high-frequency elastic wave scattering on unstructured triangular mesh grids. *Int J Numer Methods Eng* 84:330–350
- Feng X, Wu H (2011) hp-discontinuous Galerkin methods for the Helmholtz equation with large wave number. *Math Comput* 80(276):1997–2024
- Gittelsohn C, Hiptmair R, Perugia I (2009) Plane wave discontinuous Galerkin methods: analysis of the  $h$ -version. *ESAIM: Math Model Numer Anal* 43:297–331
- Graff K (1991) Wave motion in elastic solids. Dover, New York
- Guo B, Sun W (2007) The optimal convergence of the h-p version of the finite element method with quasi-uniform meshes. *SIAM J Numer Anal* 45:698–730
- Hetmaniuk U (2007) Stability estimates for a class of Helmholtz problems. *Commun Math Sci* 5:665–678
- Hiptmair R, Moiola A, Perugia I (2011) Plane wave discontinuous Galerkin methods for the 2D Helmholtz equation: analysis of the  $p$ -version. *SIAM J Numer Anal* 49:264–284
- Hiptmair R, Moiola A, Perugia I (2013) Error analysis of Trefftz-discontinuous Galerkin methods for the time-harmonic Maxwell equations. *Math Comput* 82:247–268
- Hiptmair R, Moiola A, Perugia I (2016) Plane wave discontinuous Galerkin methods: exponential convergence of the  $hp$ -version. *Found Comput Math* 16:637–675
- Hu Q, Yuan L (2014a) A weighted variational formulation based on plane wave basis for discretization of Helmholtz equations. *Int J Numer Anal Model* 11:587–607
- Hu Q, Yuan L (2014b) A plane wave least-squares method for time-harmonic Maxwell's equations in absorbing media. *SIAM J Sci Comput* 36:A1937–A1959
- Hu Q, Yuan L (2018) A plane wave method combined with local spectral elements for nonhomogeneous Helmholtz and time-harmonic Maxwell equations. *Adv Comput Math* 44:245–275
- Huttunen T, Malinen M, Monk P (2007a) Solving Maxwell's equations using the ultra weak variational formulation. *J Comput Phys* 223:731–758
- Huttunen T, Monk P (2007b) The use of plane waves to approximate wave propagation in anisotropic media. *J Comput Math* 25:350–367
- Huttunen T, Monk P, Collino F, Kaipio J (2004) The ultra-weak variational formulation for elastic wave problems. *SIAM J Sci Comput* 25:1717–1742
- Luostari T (2013) Non-polynomial approximation methods in acoustics and elasticity, Ph.D. thesis, University of Eastern Finland. Available at <https://core.ac.uk/download/pdf/19163531.pdf>
- Luostari T, Huttunen T, Monk P (2013) Error estimates for the ultra weak variational formulation in linear elasticity. *ESAIM: Model Numer Anal* 47:183–211
- Moiola A (2013) Plane wave approximation in linear elasticity. *Appl Anal* 92:1299–1307
- Moiola A, Hiptmair R, Perugia I (2011) Plane wave approximation of homogeneous Helmholtz solutions. *Z Angew Math Phys* 62:809–837
- Monk P (2003) Finite element methods for Maxwell's equation. Oxford University Press, Oxford
- Monk P, Wang D (1999) A least-squares method for the Helmholtz equation. *Comput Methods Appl Mech Eng* 175:121–136

- Peng J, Wang J, Shu S (2018) Adaptive BDDC algorithms for the system arising from plane wave discretization of Helmholtz equations, [arXiv:1801.08800v2](https://arxiv.org/abs/1801.08800v2)
- Perrey-Debain E, Trevelyan J, Bettess P (2003) P-wave and S-wave decomposition in boundary integral equation for plane elastodynamics. *Commun Numer Methods Eng* 19:945–958
- Perrey-Debain E, Trevelyan J, Bettess P (2003) Use of wave boundary elements for acoustic computations. *J Comput Acoust* 11:305–321
- Riou H, Ladevèze P, Sourcis B (2008) The multiscale VTCR approach applied to acoustics problems. *J Comput Acous* 16:487–505
- Riou H, Ladevèze P, Sourcis B, Faverjon B, Kovalevsky L (2012) An adaptive numerical strategy for the media-frequency analysis of Helmholtz's problem. *J Comput Acous* 20:1–26
- Sloane N (2000) Tables of spherical codes (with collaboration of R.H. Hardin, W.D. Smith and others) published electronically at <http://www2.research.att.com/njas/packings>
- Yuan L (2019) The plane wave discontinuous Galerkin method combined with local spectral finite elements for the wave propagation in anisotropic media. *Numer Math Theory Methods Appl* 12:517–546
- Yuan L, Hu Q (2019) Error analysis of the plane wave discontinuous Galerkin method for Maxwell's equations in anisotropic media. *Commun Comput Phys* 25:1496–1522
- Yuan L, Hu Q (2018) Comparisons of three kinds of plane wave methods for the Helmholtz equation and time-harmonic Maxwell equations with complex wave numbers. *J Comput Appl Math* 344:323–345
- Yuan L, Hu Q, Hengbin AN (2016) Parallel preconditioners for plane wave Helmholtz and Maxwell systems with large wave numbers. *Int J Numer Anal Model* 13(5):802–819
- Zhu L, Wu H (2013) Preasymptotic error analysis of CIP-FEM and FEM for Helmholtz equation with high wave number. Part II: *hp* version. *SIAM J Numer Anal* 51:1828–1852

**Publisher's Note** Springer Nature remains neutral with regard to jurisdictional claims in published maps and institutional affiliations.